Hidden variations of Alzheimer's pathology:
Insight into the amyloid diversity using conformation-sensitive dyes

Dissertation

zur Erlangung des Grades eines
Doktors der Naturwissenschaften

der Mathematisch-Naturwissenschaftlichen Fakultät
und
der Medizinischen Fakultät
der Eberhard-Karls-Universität Tübingen

vorgelegt
von

Jasmin Mahler
Heidelberg, Deutschland

September 2016

Tag der mündlichen Prüfung: 09.12.2016

Dekan der Math.-Nat. Fakultät: Prof. Dr. W. Rosenstiel
Dekan der Medizinischen Fakultät: Prof. Dr. I. B. Autenrieth

1. Berichterstatter: Prof. Dr. M. Jucker
2. Berichterstatter: Prof. Dr. T. Euler

Prüfungskommission: Prof. Dr. M. Jucker

                      Prof. Dr. T. Euler

                      Prof. Dr. M. Tolnay

                      Prof. Dr. P. Heutink

Erklärung:

Ich erkläre, dass ich die zur Promotion eingereichte Arbeit mit dem Titel:

**"Hidden variations of Alzheimer's pathology:
Insight into the amyloid diversity using conformation-sensitive dyes"**

selbständig verfasst, nur die angegebenen Quellen und Hilfsmittel benutzt und wörtlich oder inhaltlich übernommene Stellen als solche gekennzeichnet habe. Ich versichere an Eides statt, dass diese Angaben wahr sind und dass ich nichts verschwiegen habe. Mir ist bekannt, dass die falsche Abgabe einer Versicherung an Eides statt mit Freiheitsstrafe bis zu drei Jahren oder mit Geldstrafe bestraft wird.

Tübingen, den 14.09.2016

....
Unterschrift

Acknowledgements

Table of contents

Summary

The pathological aggregation of amyloidogenic proteins characterizes many neurodegenerative diseases such as Alzheimer disease (AD), which represents the most common form of dementia. The amyloid-beta (Aβ) peptide is one of the principal aggregating proteins in AD. Aβ is suggested to have the ability to adopt distinct structural conformations, a feature reminiscent of prion "strains" described for transmissible spongiform encephalopathies. *In vitro*, distinct biological activities were induced by structural differences in Aβ and distinct Aβ conformations have been described in Aβ precursor protein (APP) transgenic (tg) mouse models. Only recently the existence of structural Aβ variants has been suggested among smaller cohorts of AD patients. Nevertheless, the molecular basis for these variations could so far not be elucidated in mouse models of β-amyloidosis and the diversity of structural characteristics remains obscure in the broader population of AD patients. In this regard, the aim of this thesis was to further investigate differences in Aβ conformation. Thereby, novel conformation-sensitive dyes, called luminescent conjugated oligothiophenes (LCOs), should serve to assign a structural fingerprint to the distinct Aβ aggregates.

In a first set of experiments, we investigated the existence of different Aβ conformers in models of β-amyloidosis. Initially, we were interested in the impact of endogenous murine Aβ on amyloid formation in tg mice. APP tg mouse models develop many of the typical characteristics of β-amyloidosis due to the overproduction of human Aβ but generally continue to express endogenous murine Aβ. Even though the murine Aβ peptide is present, its contribution to the β-amyloidosis or its influence on the plaque conformation in APP tg mouse models remains to be elucidated. We detected an influence of murine Aβ on the plaque load in a slowly Aβ-depositing model, whereas no obvious effect was seen in a model with more rapid amyloidosis. While we could show a tight association of murine with human Aβ fibrils, no significant influence of the murine Aβ subtype on the Aβ plaque conformation could be detected in this study. Conclusively, the mechanistically complex interaction of the two Aβ subtypes may affect the pathogenesis of APP tg mouse models and

should be considered respectively when different models are used for translational preclinical studies. In the following, we were interested in whether distinct Aβ conformations can be detected independent of the biological system and thus investigated Aβ conformers in an organotypic slice culture model for β-amyloidosis. Aβ deposition was induced in hippocampal slice cultures (HSCs) with a combinatorial treatment of Aβ seeding extract and synthetic Aβ. Spectral analysis following LCO staining revealed conformational differences between the Aβ deposits in the cultures, shown to be dependent on both the origin of the Aβ seeding extract (from APP23 or APPPS1 tg mice) and the type of synthetic Aβ (Aβ1-40 or Aβ1-42). These experiments substantiated the feasibility of investigating conformational differences of Aβ in HSCs, a fast and easy-accessible model system that combines the advantages of *in vitro* and *in vivo* approaches to study β-amyloidosis. As a final step to further investigate the properties of Aβ as a pathogenic protein, we investigated whether the observed Aβ conformers were conserved upon formaldehyde fixation. Prions are known for their remarkable resistance to the inactivation by formaldehyde. In our study, we could show that beside the Aβ inducing activity, also the conformational differences were preserved after formaldehyde fixation. We detected different Aβ conformers between mice inoculated with fixed brain material from either APP23 or APPPS1 tg animals. These findings might be exploited to establish the relationship between the molecular structure of Aβ aggregates and the variable clinical features and disease progression of AD even in formalin-fixed autopsy material.

The second set of experiments was designed to assess conformational differences between Aβ aggregates directly in human AD tissue. Post-mortem brain tissues from 26 AD cases were investigated by spectral analysis using the conformation-sensitive LCO dyes. We were able to spectrally distinguish morphologically similar Aβ plaques from familial and sporadic AD cases. Interestingly, spectral analysis could detect differences not only within different familial cases but also within the group of sporadic AD patients, for which the origin of these variations remains mainly elusive. Structural differences in sporadic patients did not correlate with risk factors such as the age or apolipoprotein E genotype, and neither with biochemical characteristics. These

results provide evidence for the structural diversity of Aβ aggregates among AD cases with either different or related etiologies. In the future, the observed conformational variety might be further investigated and correlated to clinical data of the patients.

In conclusion, we were able to detect conformational differences between Aβ aggregates by applying a novel conformation-sensitive method. We observed distinct Aβ conformers in different models of β-amyloidosis and intriguingly also among AD patients. The variations found in AD patients may account for different neurotoxic or cognitive defects in these patients and should be further investigated in relevance to the disease. Using our findings as a foundation, a crucial goal would be to develop novel structure-specific compounds that can specifically target the harmful conformers. This would open the possibility for the development of structure-specific imaging tools applicable for diagnostics or in personalized therapies.

Introduction

1. Amyloid proteins

1.1. Definition and general overview

When the Dutch chemist Geradus Johannes Mulder first described proteins in 1839 (Mulder, 1839), he had presumably no idea how important these substances are in the human body and he could not have predicted that a century later they would also be crucial pathological entities of neurodegenerative disease. Proteins are polymers build up of long chains of amino acid residues, which are involved in nearly every process in the living organism (Branden and Tooze, 1999). They are responsible for catalysis, transport, protection, regulation, and scaffolding among other cellular tasks, which are fundamental for a healthy, well-functioning organism. However, proteins can also be harmful, if they lose their physiological function or if they gain toxic, pathogenic functions (Pallares and Ventura, 2016). A group of proteins - called amyloidogenic proteins - can exhibit a pathogenic function, because of their tendency to misfold and aggregate, which can initiate a disease process.

The term amyloid was introduced back in 1854 from the German pathologist Rudolph Virchow (Virchow, 1854, Sipe and Cohen, 2000, Kyle, 2001). Virchow observed a characteristic reaction of the cerebral corpora amylacea with iodine. He named these structures amyloid, derived from the Latin "amylum", because he was convinced that the substance he found in the corpora amylacea was starch. Though, at that time, it was still under debate whether amyloid should be considered to be starch or cellulose (Sipe and Cohen, 2000). As staining methods and microscopy techniques improved over the years, our understanding of amyloid structures has advanced considerably and a detailed overview of the amyloid structure and formation is found in the next section (see 1.2.). Nowadays, an amyloid protein is known as an insoluble, unbranched filament consisting of many-stranded β-sheets (Eisenberg and Jucker, 2012, Sipe et al., 2014). Amyloid fibrils are typically around 10 nm thick and 0.1 – 10 μm in length. By definition, all amyloids exhibit a characteristic cross-β diffraction pattern when X-rays are directed on them. Amyloid deposits have an

affinity for the dye Congo red and these red-stained deposits are birefringent, exhibiting typical green or yellow anomalous colors when examined between crossed polarizers (Howie et al., 2008, Howie, 2015). Classically amyloid deposits were characterized as being found in extracellular spaces of living tissue. Nevertheless, some intracellular deposits such as neurofibrillary tangles of the tau protein are also matching most of the biochemical characteristics and may therefore be called "intracellular amyloid" (Sipe et al., 2014). So far, approximately 25 proteins have been identified as amyloid-forming under physiological conditions. All of these amyloid proteins are associated with serious diseases including the most common age-related neurodegenerative diseases, Alzheimer`s disease (AD) and Parkinson`s disease (PD), but also the infamous Creutzfeldt-Jakob disease (CJD) caused by prions (Ross and Poirier, 2004, Chiti and Dobson, 2006, Eisenberg and Jucker, 2012). An overview of some important human amyloid diseases and associated amyloid proteins can be found in Table 1. The proteins in the amyloid state are herein designated as protein A, followed by a suffix, which is an abbreviated form of the parent or precursor protein name (Sipe et al., 2014).

Table 1. Selected human amyloid diseases and associated amyloid proteins (modified from Eisenberg and Jucker, 2012).

Disease	Amyloid protein
Alzheimer's disease	Aβ
Amyotrophic lateral sclerosis	ASOD1
Creutzfeldt-Jakob Disease	APrP
Familial British Dementia	ABri
Familial Danish Dementia	ADan
Frontotemporal lobar degeneration (FTLD)-tau	ATau
Gerstmann-Sträussler-Scheinker	APrP
Hereditary cerebral hemorrhage with amyloidosis, Dutch type	Aβ
Hereditary cerebral hemorrhage with amyloidosis, Icelandic type	ACys
Parkinson's disease	ASyn
Transthyretin familial amyloidosis	ATTR

1.2. Structure and formation

The non-crystalline and insoluble nature of amyloids for a long time caused difficulties in determining their molecular architecture by classic high-resolution structural biology methods like X-ray crystallography or nuclear magnetic resonance (NMR; reviewed in Tycko, 2015). Nevertheless, the field gained some insight into the molecular structure of amyloids over the years with more recent advanced methods including cryo-electron microscopy (Jimenez et al., 1999) or solid-state NMR (Tycko, 2011). Early electron microscopic analysis revealed that each amyloid fibril consists of two to three protofilament subunits, which are arranged in a helical manner (Shirahama and Cohen, 1967, Serpell et al., 2000, Sanders et al., 2014). In each individual protofilament, the polypeptide chain has been re-arranged into β-strands that run perpendicular to the long axis of the fibril. This arrangement of the fibrils produces the cross-β diffraction pattern when X-rays are directed on amyloids. The pattern shows two characteristic scattering diffraction signals at 4.7 and 10 Å, which result from the stacking and inter-strand distances in the β-sheets, respectively (Eanes and Glenner, 1968, Sunde et al., 1997). Already in 1935 William Astbury observed the characteristic cross-β diffraction pattern by simply holding a stretched, poached egg white into an X-ray beam (Astbury et al., 1935). Later, Pauling and Corey showed that the β-sheets in the amyloid fibrils are connected via hydrogen bonds (Pauling and Corey, 1951, Eisenberg and Jucker, 2012). The backbone C=O and N-H groups of adjacent β-strands bind to each other and form a very stable network of β-sheets that run perpendicular to the fibril axis. Neighboring β-sheets can thereby be arranged in a parallel or anti-parallel fashion (Eisenberg and Jucker, 2012). The exposure of the hydrogen bonds in the β-strand backbone and the subsequent binding to other protein chains are the prerequisites for the formation and elongation of amyloid fibrils. Amyloid formation can be initiated by the failure of the protein to maintain its native functional conformation, leading to accumulation of the protein into insoluble aggregates (Stefani and Dobson, 2003). This process can be promoted by the accumulation of partially unfolded or misfolded species, which are highly aggregation-prone or by an imbalance between protein synthesis and clearance mechanisms (Powers et al., 2009).

In vitro, the aggregation process of amyloid proteins is characterized by a slow lag phase in the beginning, followed by a fast exponential growth phase. Once an oligomeric nucleus or "seed" is formed, the aggregation process occurs quite rapidly (Jarrett and Lansbury, 1993, Chiti and Dobson, 2006, Lee et al., 2011). This nucleation-dependent mechanism of amyloid formation is graphically depicted in Figure 1. The addition of pre-formed exogenous seeds decreases the lag time of the aggregation procedure dramatically, a process called "seeding" (Walker et al., 2002, Meyer-Luehmann et al., 2006, Eisele et al., 2009).
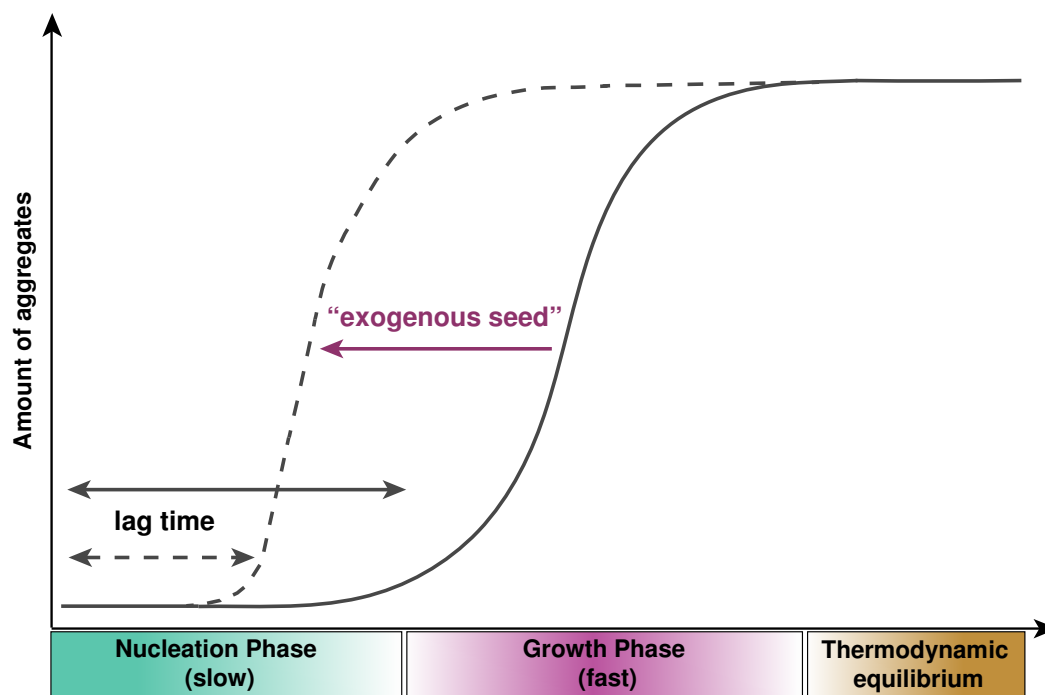
Figure 1. Nucleation-dependent formation of amyloid aggregates. The initiation of the aggregation process is characterized by a slow phase, in which an oligomeric nucleus (seed) is formed from misfolded amyloid proteins. Typically, it takes a certain time until the first aggregates are detectable, which is also called "lag time". Once the nucleus is formed, further addition of monomers happens very rapidly and larger aggregates and fibrils are formed (growth phase). At some point the growth process slows down and reaches a thermodynamic equilibrium. The addition of an exogenous seed into the system can dramatically shorten the lag time and an earlier and faster growth phase is triggered (dashed line; modified from Jarrett and Lansbury, 1993).

1.3. Amyloid diversity

Cohen and Calkins already noted in 1959 that amyloids from different sources are chemically very similar (Cohen and Calkins, 1959). Indeed, all amyloids are comprised of insoluble fibers that share a common structural build-up and

consequently exhibit a similar X-ray diffraction pattern (Sunde et al., 1997). Amyloids show a common core structural element composed of two to four β-sheets that closely interact with each other, despite potential differences in the underlying polypeptide sequences. Further, repetitive hydrophobic interactions can be often observed along the fibril axis of the amyloid polypeptide (Chiti and Dobson, 2006). Beside these similarities, a significant morphological heterogeneity can exist between amyloid fibrils, even those formed from the same peptide (Bauer et al., 1995, Tycko, 2015). Depending on the arrangement of the side chains, the length of the β-strands as well as the parallel or antiparallel arrangement can vary. Furthermore, the length and conformation of the β-sheet loops, the spacing between the β-sheets or the number of sheets that form the protofilament can be substantially different between amyloid proteins (Chiti and Dobson, 2006, Tycko, 2015). The polymorphism of amyloid fibrils can also be influenced by the growth conditions of the fibrils. Factors like the nucleation-, extension-, or fragmentation rates can determine the predominant fibril species. All above-mentioned factors can cause certain heterogeneity of amyloids that may lead to pathological differences, which underlie a specific disease. Amyloid diseases will be discussed more closely in the next chapter.

2. Amyloid diseases

2.1. Alzheimer's disease

AD is a neurodegenerative disease and the most common form of dementia. The term dementia describes a set of symptoms that includes loss of memory, mood changes as well as problems with communication, reasoning and handling daily life. Dementia is a progressive process indicating that the symptoms get gradually worse. Auguste Deter exhibited those symptoms together with disorientation and hallucinations when she was examined by Alois Alzheimer in 1901 (Alzheimer, 1907). In 1906, after Auguste Deter died, Alzheimer analyzed her brain and described a disease, which was later named after him by Emil Kraepelin (Kraepelin, 1910). Beside an overall atrophic brain, Alzheimer observed lesions resembling "senile plaques" and "neurofibrillary tangles", which are established as hallmark lesions of AD today (Figure 2;

Alzheimer, 1907, 1911, Glenner and Wong, 1984, Goedert and Spillantini, 2006). Senile plaques are extracellular deposits of the amyloid-beta (Aβ) peptide, which can be found in limbic brain regions such as the hippocampus and amygdala but also in specific cortical and subcortical regions. Classical senile plaques, show a central compact core structure enriched in Aβ that can be specifically stained by Congo red and is often surrounded by more loosely arranged Aβ deposits and dystrophic neurites (Masters et al., 1985, Morgan et al., 2004). However, in most AD cases, less dense and mainly Congo red-negative Aβ deposits are much more abundant, which are often referred to as "diffuse" Aβ plaques (Tagliavini et al., 1988, Morgan et al., 2004). Neurofibrillary tangles are filamentous lesions composed of hyperphosphorylated forms of the microtubule-associated protein tau that accumulates in selective neurons in the brains of AD patients (Kosik et al., 1986).
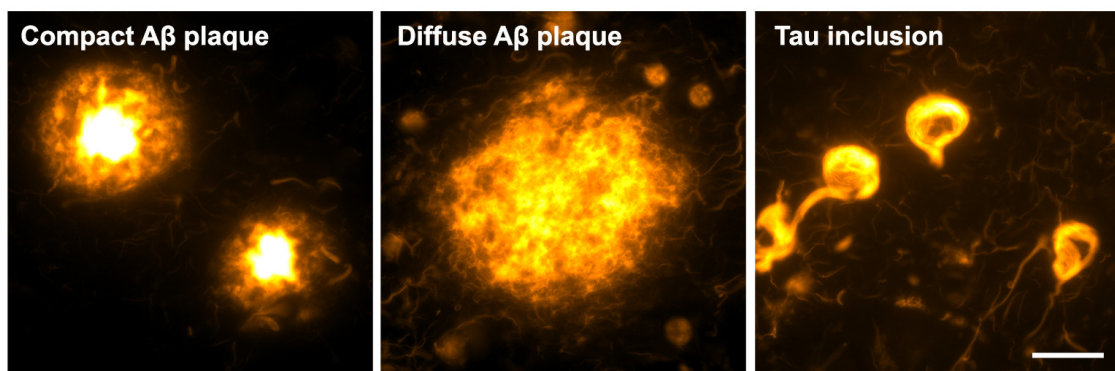
Figure 2. Hallmark lesions of AD. Extracellular deposits of Aβ can be found as compact or diffuse aggregates in the brains of AD patients. Representative pictures show compact and diffuse Aβ plaques fluorescently labeled with an amyloid-specific dye. Intracellular tau inclusions constitute the second hallmark pathology of the disease. A representative picture shows fluorescently labeled neurofibrillary tangles made of tau protein in human AD brain sections. Scale bar: 20 µm.

In the beginning of the 20th century, when Alzheimer made his observations, life expectancy was much shorter than it is today, and with age as the highest risk factor for AD (Yoshitake et al., 1995, Alzheimer's-Association, 2015), it was a rather rare disease. As of 2015, there were approximately 9.9 million new cases of dementia worldwide, which means one new case every three seconds (Prince et al., 2015). The total number of cases reached thereby an estimated 46.8 million people last year and this number is expected to almost double every 20 years. Some studies are more optimistic, indicating that the age-

specific risk of AD and other dementias in higher-income western countries may even have declined in the past 25 years (Manton et al., 2005). These declines have largely been attributed to higher levels of education and improved control of cardiovascular risk factors (Schrijvers et al., 2012). In addition to the medical issues, a high number of dementia cases also means a considerable economical burden for the whole society (Alzheimer's-Association, 2015). The global costs for dementia are at present approximately US$ 818 billion and they increase steadily (Prince et al., 2015). This proves especially dramatic in low or middle-income countries, which harbor more than half of all dementia cases. Notably, some of the cases that contribute to the numbers listed above might not suffer solely from AD, but may harbor other pathologies. Some scientists even view AD as a heterogeneous syndrome, essentially a collection of many diseases, whereas others see it as a homogenous disorder with ageing contributing minor aspects (Morris et al., 2014). Conclusively, AD is an incurable and devastating disease, which causes tremendous problems and encumbrances for patients and caregivers and in addition it constitutes a substantial global financial challenge. In this regard, it is of great interest for our society to interfere with this high numbers of AD cases worldwide and to find an effective treatment strategy.

2.2. APP processing and the Aβ peptide

The main actor in AD is the Aβ peptide. It is derived from the Aβ precursor protein (APP) through sequential secretase-mediated cleavage steps (Figure 3; Sisodia et al., 1990, Sisodia, 1992, Thinakaran and Koo, 2008). APP constitutes a single-pass transmembrane protein, which is produced in large quantities in neurons and is metabolized very rapidly (O'Brien and Wong, 2011). In 1987, several groups determined experimentally that the gene encoding APP is located on chromosome 21 and therefore provided the missing link between AD and Down's syndrome (trisomy 21; Goldgaber et al., 1987, Kang et al., 1987, Robakis et al., 1987). The pathway of APP processing can either follow a "non-amyloidogenic" route (Figure 3A), which doesn't result in Aβ production, or it can follow the "amyloidogenic" route leading to Aβ generation and finally AD (Figure 3B). In the non-amyloidogenic pathway, APP is first cleaved by α-

secretase within the sequence of Aβ thereby preventing Aβ production (Esch et al., 1990, Sisodia et al., 1990, Sisodia, 1992). The extracellular secreted fragment of APP that is produced is called APPsα and the remaining membrane-bound c-terminal fragment (CTF), called CTF-α. A cut by γ-secretase (composed of at least four subunits including the proteins presenilin 1 or 2, nicastrin, APH-1 and PEN-2; Edbauer et al., 2003, Chow et al., 2010), cleaves the CTF-α subsequently into the APP intracellular domain (AICD) and p3. In contrast, the amyloidogenic pathway leads to Aβ production through sequential cleavage by β-secretase and γ-secretase. In the first step, β-secretase cutting generates the secreted APPsβ fragment and the membrane-bound CTF-β. Finally, CTF-β is processed by cleavage through the γ-secretase into AICD and the Aβ peptide. The latter may subsequently form Aβ fibrils and aggregate into pathogenic Aβ plaques as depicted in Figure 3.
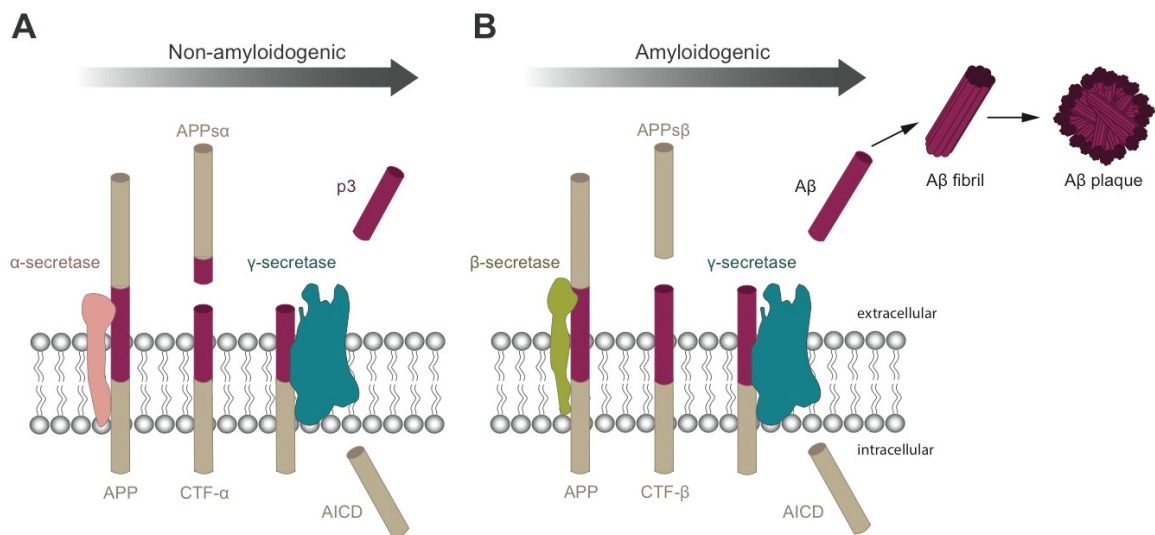
Figure 3. APP processing and related pathways. **(A)** In the non-amyloidogenic pathway, APP is sequentially processed by membrane-bound α- and γ-secretases. α-secretase cleaves within the Aβ domain, thus precluding generation of an intact Aβ peptide. The fates of N-terminally truncated Aβ (p3) and the APP intracellular domain (AICD) are not fully determined. **(B)** The amyloidogenic processing of APP is carried out by sequential action of membrane-bound β- and γ-secretases. The resulting Aβ peptide gets secreted into the extracellular space where it tends to aggregate and form Aβ fibrils and plaques (modified from Thinakaran and Koo, 2008).

The length of the generated Aβ can range from 38 to 43 amino acids, whereby the predominantly produced peptide is 40 amino acids long (Aβ40) (Vigo-Pelfrey et al., 1993). This variability depends on the exact cleavage site of the γ-secretase. Aβ isoforms ending at amino acid 42 (Aβ42) have been shown to be

the most aggregation-prone, constituting one of the determining factors of amyloid formation (Jarrett et al., 1993). In the recent years, numerous shorter isoforms of Aβ have been detected in the brains of AD patients (Tekirian et al., 1998, Portelius et al., 2008), although the relative importance of these truncated isoforms in the pathogenesis of AD remains controversial (Portelius et al., 2010b).

2.3. Genetics of Alzheimer's disease

Glenner and Wong identified the Aβ amino acid sequence in 1984 by extracting cerebrovascular amyloid from dementia patients (Glenner and Wong, 1984). Together with subsequent analyses performed by Hardy and colleagues in the early 1990's, the way was paved for the main hypothesis about the successive events leading to AD. The "amyloid cascade hypothesis" regards Aβ accumulation as the hallmark event, followed by further neurological changes such as neurofibrillary tangle formation or synapse loss (Hardy and Allsop, 1991, Hardy and Higgins, 1992, Hardy and Selkoe, 2002). Thereby, Aβ aggregation is seen as a consequence of the misbalance between Aβ production and Aβ clearance. Strong support for the amyloid cascade hypothesis is given by the familial forms of AD (FAD), which are mainly caused by mutations in genes involved in Aβ metabolism. FAD will be discussed more closely in the next section (see 2.4.). Interestingly, the majority of patients, about 99%, suffer from late-onset sporadic AD (SAD; Goedert and Spillantini, 2006). The cause for SAD is mainly unknown, although several factors were identified that might influence the risk to develop AD or lower the age of disease onset. Among those, age is the highest risk factor for AD, but also diabetes, atherosclerosis, head-injury and a number of behavioral and environmental factors (Mayeux, 2003). The best-established risk factor for SAD is apolipoprotein E (ApoE), which is a secreted lipoprotein involved in cholesterol metabolism. ApoE was discovered as a genetic risk factor for SAD in 1993 (Corder et al., 1993) and it exists as three isoforms ApoE2, ApoE3 and ApoE4. The possession of one or two copies of ApoE4 increases AD risk up to 12-fold relative to ApoE3, while the rare ApoE2 allele is even protective (Corder et al., 1993, Strittmatter et al., 1993, Holtzman et al., 2012). The ApoE4 effect is found

in various populations and marked by an earlier disease onset with more severe pathology, but otherwise typical clinical progression.

2.4. From familial Alzheimer's disease to models of β-amyloidosis

Molecular genetics studies in several affected families have identified three main genes associated with highly penetrant early-onset FAD: the APP gene on chromosome 21 (Van Broeckhoven et al., 1990, Goate et al., 1991), presenilin 1 (PSEN1) on chromosome 14 (Sherrington et al., 1995) and presenilin 2 (PSEN2) on chromosome 1 (Levy-Lahad et al., 1995). To date, over 230 mutations in PSEN1 are known to be involved in FAD, making it the most common cause of the hereditary forms of the disease (www.alzforum.org/mutations). The mutations in both PSEN genes influence the APP processing to yield preferentially Aβ42, thereby increasing the Aβ42/40 ratio (De Strooper, 2007). Most pathogenic APP mutations cluster near the β-secretase and γ-secretase cleavage sites (Figure 4). Generally, these mutations increase total Aβ levels and/or the Aβ42/Aβ40 ratio as shown in cell culture experiments (Haass et al., 2012), while APP promoter mutations and APP gene duplication have the same effect. Other mutations in APP are associated with rare cases of familial vascular amyloidosis. FAD patients show the first signs of dementia often before 60 years of age and the disease is generally autosomal dominantly inherited (Selkoe, 2011). An overview of familial mutations causative for AD is presented in Figure 4.
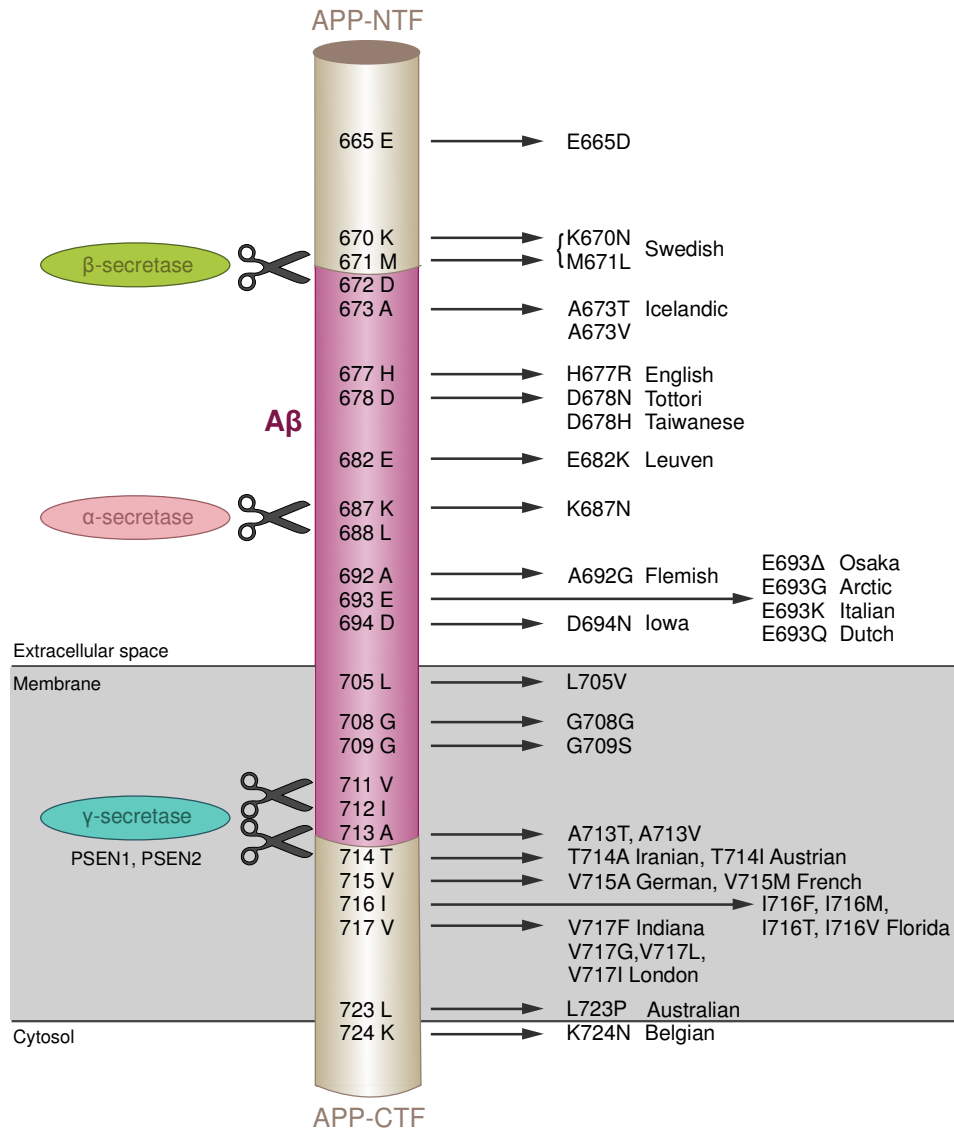
Figure 4. APP mutations associated with familial AD (FAD). Mutations associated with early-onset FAD are highlighted in part of the amino acid sequence of APP. Most mutations are clustered in the close vicinity of secretase-cleavage sites, thereby influencing APP processing. The mutations are named after the nationality or location of the first family in which that specific mutation was demonstrated. Familial mutations in the presenilin 1 and 2 genes (PSEN1, PSEN2) are influencing γ-secretase processing. The Aβ sequence is indicated in dark red (modified from Van Dam and De Deyn, 2006).

The FAD cases included in this thesis carry mutations in the APP or PSEN1 genes. Some details about these mutations are found in the following:

APP V717I

The V717I mutation in APP was discovered in a patient from the English capital and is therefore called the "London" mutation (Goate et al., 1991, Hardy et al.,

1991). It was one of the first described mutations for APP and is the most common APP mutation worldwide. The average age-of-onset in these patients lies between 50-60 years. Neuropathologically, the phenotype associated with this mutation is highly variable. Besides severe AD pathology, amyloid angiopathy and Lewy bodies are often observed (www.alzforum.org/mutations). The APP V717I mutation is part of a group of mutations clustering around the γ-secretase cleavage site. As confirmed in cell culture experiments, this mutation increases the Aβ42/40 ratio by increasing the Aβ42 levels while Aβ40 stays unaffected (Eckman et al., 1997).

PSEN1 A431E

The A431E mutation in PSEN1 is frequently found in FAD cases with Mexican origin and genetic analyses hint to a founder mutation descending from a single common ancestor (Rogaeva et al., 2001, Murrell et al., 2006, Yescas et al., 2006). Characteristic for this mutation is a very early onset of the disease, often before 40 years of age. The neuropathology shows cotton wool plaques along with classical AD pathology. Mutation carriers are shown to have low levels of Aβ1-37, Aβ1-38 and Aβ1-39 fragments, which are produced by the γ-secretase. This indicates, that the mutation might modulate γ-secretase cleavage in a disease-promoting manner (Portelius et al., 2010a).

PSEN1 F105L

The F105L mutation in PSEN1 was first discovered in a patient from Germany (Finckh et al., 2000). The onset of the disease seems to range between 50-60 years of age, although only a few affected families have been identified so far. In addition to AD pathology, those patients often show signs of Parkinsonism. So far, the biological effects of this mutation are unknown (www.alzforum.org/mutations).

Based on the knowledge about the familial mutations, animal models for different amyloid pathologies were generated. Genetically modified animals harboring these disease-associated mutations reproduce some, whereby not all aspects associated with AD (Jucker, 2010). Two well-studied transgenic (tg) mouse models for cerebral β-amyloidosis, both characterized by high Aβ

production, are the so-called APP23 and APPPS1 mice. APP23 mice harbor the "Swedish" double-mutation KM670/671NL in APP (Sturchler-Pierrat et al., 1997) which is located immediately adjacent to the β-secretase cleavage site (see Figure 4; Mullan et al., 1992). This mutation results in an enhanced cleaving capacity of the β-secretase leading to an increased total Aβ production (Sturchler-Pierrat et al., 1997). The APPPS1 mice express in addition to the Swedish double-mutation, human PSEN1 with the L166P mutation resulting in an increased ratio of Aβ42 over Aβ40 (Radde et al., 2006). Currently, mouse models are the best-established system to study human age-related neurodegenerative diseases (Jucker, 2010). In summary, AD manifests as a genetically heterogeneous disease with familial and sporadic etiologies. Mouse models engineered to recapitulate aspects of amyloid pathology contribute to the better understanding of mechanisms involved in AD.

3. Amyloid conformers

3.1. Prion strains

Classically, prions are defined as infectious particles consisting of misfolded prion protein (PrP; Prusiner, 1982, Prusiner, 1998). Prions can cause fatal transmissible diseases in mammals including humans. Among them is the variant CJD representing a unique human form of bovine spongiform encephalopathy (BSE) known in cattle. Besides the aggregation of PrP, prion diseases are pathologically characterized by spongiform degeneration of the brain and neuronal loss (DeArmond and Prusiner, 1995). Similar to other amyloid diseases, there can be either hereditary or idiopathic forms. The pathogenic agent in prion disease is a misfolded isoform of the normal, cellular PrP (PrP^c), called PrP-scrapie (PrP^{Sc}). PrP^{Sc} is abnormally enriched in β-sheets and can induce other PrP molecules to misfold and aggregate (Prusiner, 1998, Prusiner, 2013). PrP^{Sc} shows resistance to denaturation, partial resistance to protease digestion and is quite insoluble (Cohen and Prusiner, 1998). Furthermore, PrP^{Sc} seems to be very resistant to the inactivation by formaldehyde, a chemical used for the fixation of tissues and to neutralize viruses during the preparation of vaccines (Fox et al., 1985, Delrue et al., 2012). Certain variability is observed in the clinical and pathological occurrence of

prion diseases. These variations are based on differences in conformation and arrangement of the underlying proteins and are referred to as prion "strains" (Aguzzi et al., 2007, Collinge and Clarke, 2007, Prusiner, 2013). Many factors, such as post-translational modifications and specific aggregation conditions can create distinct self-propagating conformations of PrP^{Sc} giving rise to different prion strains (Safar et al., 1998, Frost and Diamond, 2010). After inoculation into tg animals, prion strains cause consistent disease characteristics, such as a specific incubation period, distinct patterns of PrP^{Sc} distribution and a certain severity of the spongiosis in the brain. Typically, bioassays are applied that identify a successful transmission of prion strain characteristics into a new host to define different strains (Aguzzi et al., 2007, Collinge and Clarke, 2007).

3.2. Conformational differences of other amyloids

The concept of strains is not restricted to prions but rather seems to be a common characteristic of amyloid diseases (Chiti and Dobson, 2006, Tanaka et al., 2006, Walker and Jucker, 2015). For example, distinct Aβ fibrils can be formed by seeded fibril growth presenting with different conformations and toxicities, which are even passed to the next generation of fibrils (Petkova et al., 2005). Seeding studies in tg mice showed that Aβ seeds derived from tg mouse models for cerebral amyloidosis or human AD tissue can be transmitted to APP tg host mice inducing an accelerated pathology (Walker et al., 2002, Meyer-Luehmann et al., 2006, Eisele et al., 2009, Eisele et al., 2010, Langer et al., 2011, Eisele et al., 2014). Intriguingly, differences in molecular composition and conformation of the Aβ seeds are maintained after propagation in the host mice (Heilbronner et al., 2013). Similar to Aβ, prion-like induction is also seen for intracellular amyloid proteins like tau inclusions or α-synuclein (α-syn), the main aggregating protein in PD (Frost and Diamond, 2010, Goedert et al., 2010). For tau, a recent study revealed that different tau strains induce differential patterns of induction and microglia activation in the brains of tau tg mice (Sanders et al., 2014). Furthermore, the injection of homogenized brain material from patients with distinct tauopathies into tg mice produced morphologically different tau inclusions (Clavaguera et al., 2013). In the case of α-syn, missense mutations, which are responsible for dominantly inherited forms of PD, give rise to fibrils

whose conformation is distinct from that of wild-type (wt) fibrils (Yonetani et al., 2009). Distinct α-syn fibril structures can even cross-seed tau fibrils differentially as shown *in vitro* and in tg mouse studies (Guo et al., 2013). Finally, it was proven that conformationally different α-syn strains are able to induce distinct histopathological and behavioral phenotypes, reminiscent of prion strains (Peelaerts et al., 2015). In summary, Aβ, tau and α-syn exhibit prion-like templated misfolding, as shown by *in vitro* studies and in tg mouse models. Similar to prions, these proteins might also form distinct conformers in humans that account for differences in the pathogenic phenotype of the diseases. Although Lu et al. lately identified a single distinct Aβ fibril structure in each of two AD patient brains (Lu et al., 2013), the link between the underlying conformation and the clinical phenotype was not conclusive. It is still challenging to assess and compare conformational differences between amyloids and relate them to clinical variability. Thus, we have pursued a novel approach to investigate conformational differences within the fibril organization in the aggregates, by employing a novel class of amyloid dyes. Structural changes, otherwise invisible by conventional methods, manifest as a shift in the dye emission properties, which can be detected and analyzed using light microscopy techniques.

4. Novel dyes to assess amyloid conformation

4.1. Luminescent conjugated oligothiophenes (LCOs)

For decades, the dye Congo red was seen as the gold standard of amyloid detection in post-mortem brain tissues (Bennhold, 1922, Puchtler, 1962). Up to date, amyloid pathologies are still diagnosed using Congo red staining, which exhibits birefringence accompanied by yellow/green anomalous colors between crossed polarizers, as part of the classic definition of ordered structures within amyloid proteins (Sipe et al., 2014). The fluorescent Thioflavin T (ThT) is another well-established amyloid-binding dye often applied in *in vitro* amyloid fibrillation assays (Vassar and Culling, 1959, LeVine, 1993). Meanwhile, many fluorescent and non-fluorescent amyloid-specific dyes have been developed, which are often direct derivatives of the classical dyes. Such an example is the fluorescent dye Methoxy-X04, a derivate of Congo red, which has the

advantage of a better blood-brain barrier (BBB) passage upon systemic injection and is therefore often used for *in vivo* multiphoton microscopy in mouse models of AD (Klunk et al., 2002, Hefendehl et al., 2011). Another example is the Pittsburgh compound B (PIB), an analogue of ThT, which is routinely used for AD diagnosis in positron emission tomography (PET) scans in humans (Klunk et al., 2004). Although all these dyes reliably detect amyloid deposits, they do not reveal any fine molecular differences, which underlie the previously described heterogeneity in amyloid conformation. A novel group of amyloid binding dyes, the **l**uminescent **c**onjugated **o**ligo- or **p**olythiophenes (LCOs or LCPs), exhibit conformation-specific properties that could be used to examine this heterogeneity. The use of conformation-sensitivity in biological applications is not entirely new. In 1999, conjugated polymers were established as fluorescent sensors and applied for example to detect solid-state DNA (Leclerc, 1999). A conformation-dependent color reaction reported on the single or double-stranded condition of the DNA. This effect is based on the fact that the planar and non-planar conformations of the conjugated polymer have different emission spectra (Leclerc, 1999, Ho et al., 2002). Peter Nilsson and co-workers further developed this concept and established a flexible thiophene backbone as the basic principle of LCO and LCP function (Figure 5; Aslund et al., 2009a).
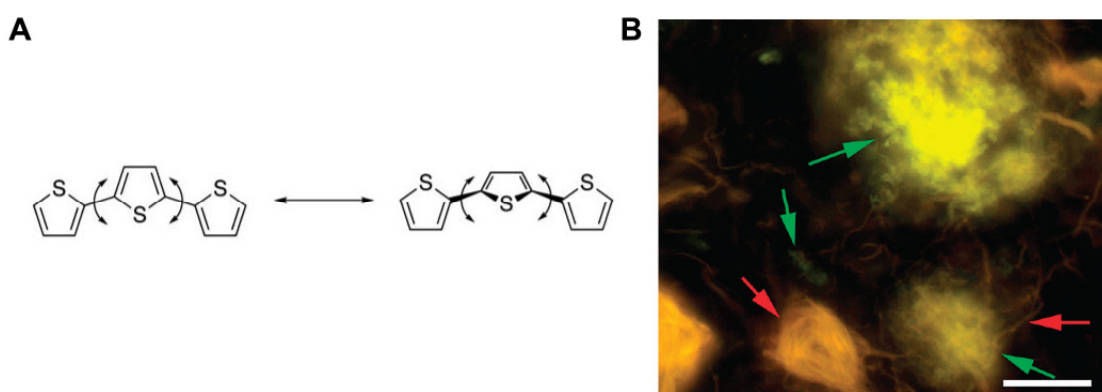
Figure 5. LCO and LCP principle of function. **(A)** The flexible LCO/LCP backbone. Binding of a LCO or LCP molecule to an amyloid protein can induce a twist in the thiophene backbone, which is dependent on the amyloid conformation. **(B)** The twisting of the LCO/LCP backbone is reflected in differences in the emission spectrum of the respective dye. High-resolution fluorescence images show the details of the interplay between Aβ deposits (green), neurofibrillary tau tangles, and dystrophic neurites (yellow red) after LCO staining. Conformationally different amyloid deposits are highlighted (green and red arrows, respectively) to indicate striking spatial co-localization and differences in emission color. Scale bar: 10 μm. Images adapted from (Aslund et al., 2009a, Aslund et al., 2009b).

They first introduced a zwitterionic LCP, which was able to visualize differences in the conformational state of synthetic peptides in 2003 (Nilsson et al., 2003). This work provided the foundation for the LCPs and LCOs to be applied for optical fingerprinting of conformationally different amyloid proteins. Two years later, the monomer-based LCP polythiophene acetic acid (PTAA) was shown to distinguish between the native and fibrillar form of insulin (Nilsson et al., 2005). The conformational changes of the protein induced during the amyloid fibrillation pathway altered the geometry of the PTAA backbone and could be observed as shift in the emission spectrum. In comparison with native insulin, the emission maximum of PTAA when added to insulin fibrils was shifted to longer wavelengths and showed decreased intensity. This shift indicated that the interaction with fibrils resulted in a planar and highly conjugated polymer backbone. Ideally, polythiophenes that are applied for amyloid detection and discrimination should only detect fibrillar protein conformations and not, as PTAA, show an optical response also when interacting with the native form. Therefore, trimer-based LCPs were engineered, which show significantly increased binding specificity for amyloid-like fibrils (Aslund et al., 2007). The superiority of these newly developed amyloid dyes to the conventional is their potential to discriminate between various amyloid conformations in disease-associated tissue by providing a direct link between spectral signature and protein conformation (Nilsson et al., 2006, Nilsson and Hammarstrom, 2008). Indeed, LCPs could be used to distinguish between different prion strains, otherwise indistinguishable by classical immunohistochemistry (Sigurdson et al., 2007). Since identical recombinant PrP exhibited indistinguishable LCP spectra in this study, the conclusion was that the characteristic differences observed on the tissue resulted from distinct conformations of the PrP strains. Similarly, LCPs can be applied for spectral discrimination of different Aβ conformations *in vitro* and in APP tg mice (Nilsson et al., 2007). LCPs have shown great potential as amyloid imaging agents (Nilsson and Hammarstrom, 2008), but at the same time some major drawbacks came to light. Dependent on the overall charge of the LCPs, very specific buffer systems are required, impeding the possibility of using them in living organisms. (Aslund et al., 2009a, Klingstedt and Nilsson, 2012) Furthermore, the inherently large molecular weight of the polymers precluded passage over the BBB. Therefore, modifications of the probe design

were required in order to optimize amyloid binding at physiological conditions and to increase the chance of BBB crossing. The solution was a well-defined shorter backbone, resulting in the LCOs (Aslund et al., 2009b). By now, many LCOs have been proven capable of distinguishing tau inclusions from Aβ pathology in mouse models of amyloidosis and post-mortem AD brain tissue (Aslund et al., 2009b, Klingstedt et al., 2011, Wegenast-Braun et al., 2012, Simon et al., 2014). Lately, a combination of two structurally different but related LCOs could even enhance the spectral differentiation since the dyes bind on separate ultra-structural elements (Nystrom et al., 2013). The tetrameric oligothiophene qFTAA was shown to respond to mature amyloid fibrils, whereas the heptameric oligothiophene hFTAA stained additionally early prefibrillar states of amyloid. Nevertheless, the relation between the conformational differences of the amyloid proteins and a potential role in the pathogenesis or diagnosis of neurodegenerative disease is still widely missing. Using this novel conformation-sensitive method, this thesis aimed to study the effect of structural diversity of amyloid aggregates on AD pathology. Thereby our goal was to gain insights into the conformation and diversity of amyloid deposits, which are not conceivable with conventional methods.

Materials and Methods

1. Mice

A variety of mouse models were used to analyze conformational differences between amyloid deposits. Hemizygous APP23 mice, overexpressing human APP with the Swedish double mutation (Sturchler-Pierrat et al., 1997) and hemizygous APPPS1 mice, co-expressing human APP with the Swedish double mutation and human PSEN1 with the L166P mutation (Radde et al., 2006) were analyzed. In addition, to investigate the influence of murine Aβ on amyloid deposition, these mice were bred with mice lacking endogenous murine APP (Calhoun et al., 1999) to generate littermates with and without the murine form (koAPP23, koAPPPS1). All mice were bred on a C57BL/6J background and all lines expressed the transgenes under the neuron-specific murine Thy1 promoter. Any procedures with animals were performed in compliance with protocols approved by the local animal use committee and university regulations.

2. Patient samples

Tissue samples from 26 clinically and pathologically diagnosed AD cases were analyzed (Table 2). Included among them were eight FAD cases (AD 1-8) with following mutations: V717I in APP, A431E in PSEN1 and F105L in PSEN1. The remaining 18 cases (AD 9-26) had a sporadic etiology.

Table 2. Case list

Case	Etiology	Age	Sex	PMI (h)	ApoE type
AD1	APP V717I	45	m	4	n.a.
AD2	APP V717I	49	f	2.7	3/3
AD3	APP V717I	54	f	5.3	3/3
AD4	PSEN1 A431E	43	f	4	3/3
AD5	PSEN1 A431E	47	n.a.	n.a.	3/3
AD6	PSEN1 A431E	44	m	n.a.	3/3
AD7	PSEN1 F105L	68	f	36	2/3
AD8	PSEN1 F105L	67	f	8	2/3
AD9	sporadic	80	f	25.8	n.a.
AD10	sporadic	62	m	8.5	2/3
AD11	sporadic	81	f	17.7	3/3
AD12	sporadic	70	m	8.5	3/3
AD13	sporadic	81	f	n.a.	3/3
AD14	sporadic	81	f	2	3/3
AD15	sporadic	62	f	6	3/3
AD16	sporadic	74	m	2.5	3/3
AD17	sporadic	54	m	5.5	3/3
AD18	sporadic	91	f	3	3/3
AD19	sporadic	81	m	4	3/3
AD20	sporadic	89	m	49	3/4
AD21	sporadic	64	m	9	3/4
AD22	sporadic	87	f	6	3/4
AD23	sporadic	58	f	6	3/4
AD24	sporadic	77	m	6	3/4
AD25	sporadic	88	m	9	3/4
AD26	sporadic	72	f	3	3/4

f = female; m = male
PMI (h) = Postmortem interval (hours)
ApoE type = Apolipoprotein E genotype

The samples were obtained from two different sources, the Emory University Brain Bank and the Indiana Alzheimer's Disease Centre. Informed consent was received from all individual participants included in the analysis.

3. Histology

Tissue for immunohistochemistry was immersion-fixed in 4% paraformaldehyde (PFA) in phosphate-buffered saline (PBS), subsequently cryoprotected in 30%

sucrose in PBS and frozen in methylbutane on dry ice. Fixed mouse brains were cut with a freezing-sliding microtome into either 25 µm or 40 µm thick sections. The sections were collected in cryoprotectant (35% ethylene glycol, 25% glycerol in PBS) and stored at -20 °C until use. Fresh frozen human tissue was cut into 12 µm thick sections on a cryotome, dried at room temperature (RT) over night and stored at -80 °C.

4. Immunohistochemistry

Immunohistochemical staining was performed according to standard immunoperoxidase procedures using an Elite ABC kit (Vector Laboratories, Burlingame, CA) and the Vector SG as a substrate. In general, Aβ deposits were stained using the polyclonal antibody CN3 (1:1000) raised against synthetic human Aβ1–16 peptide (Eisele et al., 2010). Counterstaining with Congo red was performed according to standard protocols. For immuno-labeling of murine Aβ a customized protocol was used. Unspecific binding sites were blocked in three steps: first with anti-mouse blocking serum (Vector Laboratories M.O.M. blocking reagent), second with skim milk powder (3% (w/v) solution in dH$_2$O), and third with standard blocking solution (0,15% (v/v) Triton x-100 and 5% (v/v) horse serum in Tris-buffered saline). The murine Aβ-specific monoclonal antibody m3.2 (Morales-Corraliza et al., 2009) was used as primary antibody (1:500). The anti-mouse biotinylated secondary antibody (Vector Laboratories, Vectastain mouse IgG; 1:250) was detected with a streptavidin based fluorescent detection system (ATTO647N, ATTO-Tec GmbH, Siegen, Germany; 1:500).

5. LCO staining

Three different LCO variants, qFTAA (quadro-formyl thiophene acetic acid), pFTAA (penta-formyl thiophene acetic acid) and hFTAA (hepta-formyl thiophene acetic acid) were used in this thesis for detection and analysis of amyloid pathology. pFTAA staining (3 µM in PBS) for mouse brain sections and slice cultures was performed as previously described (Klingstedt et al., 2011). The sections were incubated with the LCO solution for 30 min at RT, in a dark chamber. For the analysis of Aβ plaques in AD patients, the human tissue was stained with qFTAA and hFTAA (2.4 µM qFTAA and 0.77 µM hFTAA in PBS; 30 min RT in the dark) similar to a previous description (Nystrom et al., 2013). All

LCOs were kindly provided by K. Peter R. Nilsson, Linköping University, Sweden.

6. Image acquisition

Fluorescent and brightfield images were acquired on a Zeiss Axioplan 2 microscope with an Axiocam HRm (Carl Zeiss MicroImaging GmbH, Jena, Germany) using the respective objective (x4 objective 0.1 numerical aperture (NA) for mosaic overview pictures; x20 objective 0.5 NA, x40 objective 1.3 NA or x63 objective 1.4 NA for higher resolution imaging, all from Zeiss) and the Zeiss AxioVision 4.7 software. Images depicting pFTAA-/immuno-double labeling were taken with a Zeiss LSM 510 META (Axiovert 200M) confocal microscope. Laser lines 458 nm and 633 nm were used to excite pFTAA and ATTO647N, respectively. To depict the whole structure of interest, some images were acquired as z-stacks and maximum intensity projections are shown as indicated.

7. Spectral analysis

Spectra for all experiments were acquired on the Zeiss LSM 510 META confocal microscope using the argon 458 nm laser line for excitation; acquisition of emission spectra from 470 nm to 695 nm was performed using the Zeiss LSM META detector. For imaging of fixed mouse sections and slice cultures an x63 objective (oil-immersion, 1.4 NA, Zeiss) was used and for imaging of human Aβ deposits an x40 (oil-immersion, 1.3 NA, Zeiss) objective. For all experiments the amyloid deposits were randomly chosen and three regions of interest were measured in the center of each deposit. Care was taken to exclude areas of incomplete staining or lipofuscin autofluorescence. After the spectral measurements, all emission spectra were normalized to their respective maxima. For each deposit, the mean was calculated before averaging the values per animal or patient. The ratio of the intensity of emitted light at the blue-shifted portion and red-shifted peak was used as a parameter for spectral distinction of different Aβ deposits. In each experiment the peaks were selected individually to maximize the spectral distinction.

Spectral analysis of Aβ plaques in APPPS1 and koAPPPS1 mice: Fixed APPPS1 and koAPPPS1 mouse sections were analyzed from five mice per genotype. 14-16 Aβ plaques were investigated in each animal.

Spectral analysis of Aβ deposits in slice cultures: For the analysis of Aβ deposits in slice cultures, plaques were selected from the intermediate sections of the cultures (neither top nor bottom section) and border regions were excluded. In 11-13 cultures per treatment condition, each 4-15 Aβ plaques were analyzed.

Spectral analysis of Aβ plaques in fresh frozen and fixed mouse brain sections: APPPS1 and APP23, fresh-frozen and formaldehyde fixed brain sections were analyzed (n=3-4 animals per group). In each animal 40 Aβ plaques were measured in the hippocampus.

Spectral analysis of human AD plaques: For the analysis of human AD tissue, Aβ plaques from temporal, frontal and occipital cortices were analyzed. 15-75 Aβ plaques were measured in each of the different regions and 45-190 plaques in total per patient.

8. Stereological analysis

The Aβ loads in APP and koAPP tg mice were quantified on a CN3 and Congo red-stained set of every 12th systematically sampled coronal section. Cortical brain regions were defined using a standard mouse brain atlas. Stereological analysis was performed using a Zeiss microscope (Axioskop) equipped with a motorized xyz-stage coupled to a video-microscopy system (Microfire, Optronics, California, USA). The investigators who performed the analysis were blind to the sample genotypes. The total Aβ load (expressed as percentage of total cerebral cortex area) was determined by calculating the areal fraction occupied by CN3- and Congo red-positive staining in two-dimensional sectors (20x objective, 0.45 NA; Calhoun et al., 1998).

Results

1. Aβ conformers in models of β-amyloidosis

1.1. Human and murine Aβ subtypes in APP transgenic mouse models

This section summarizes results from the published manuscript (Mahler et al., 2015).

Mouse models of cerebral β-amyloidosis develop the typical disease-associated amyloid lesions due to the overproduction of human Aβ and generally, those mice also continue to express endogenous murine Aβ. It was shown before that both peptides deposit in these models (van Groen et al., 2006b), however the exact role of murine Aβ in amyloid formation is still elusive. The murine and human Aβ peptides differ in three amino acids at residues 5, 10 and 13 (Yamada et al., 1987). Hence, the two subtypes may contribute differentially to the amyloidosis in mouse models of AD. To this end, the influence of murine Aβ in APP23 and APPPS1 mice on a wt versus a murine APP-null background (koAPP) was analyzed.

First, the contribution of murine Aβ to amyloid deposition was assessed in both mouse lines. Looking at the APP23 versus koAPP23 mice, no obvious differences were visible with respect to amyloid deposition on anti-Aβ immunostained cortical brain sections at first glance (Figure 6A). This observation is in accordance with a previous report (Calhoun et al., 1999). However, stereological analysis of the total Aβ-positive area revealed a difference between genotypes, with APP23 mice exhibiting a ~25% increase in Aβ load compared to age-matched koAPP23 mice at 14.5 and 18.5 months of age, which reached significance for the 14.5 month-old group (Figure 6A). In addition to an increase of the diffuse and compact Aβ deposits in the brain parenchyma, an increase (~50%) in vascular Aβ (cerebral β-amyloid angiopathy, CAA) was observed for APP23 versus koAPP23 mice at both ages. Notably, CAA was only a minor component of the respective total Aβ load.

When looking at the results from the APPPS1 mice, a model of more rapid amyloidosis, no such effect was visible (Figure 6B). Although this model has lower human APP overexpression than APP23 mice (three- versus seven-fold), the onset of amyloidosis is much faster due to an increased Aβ42/40 ratio. CAA deposits are rather rare in these animals (Radde et al., 2006). Stereological analysis of the total Aβ-positive area showed only small, non-significant differences between the animals with or without the murine APP gene at 3 or 6 months of age (Figure 6B).
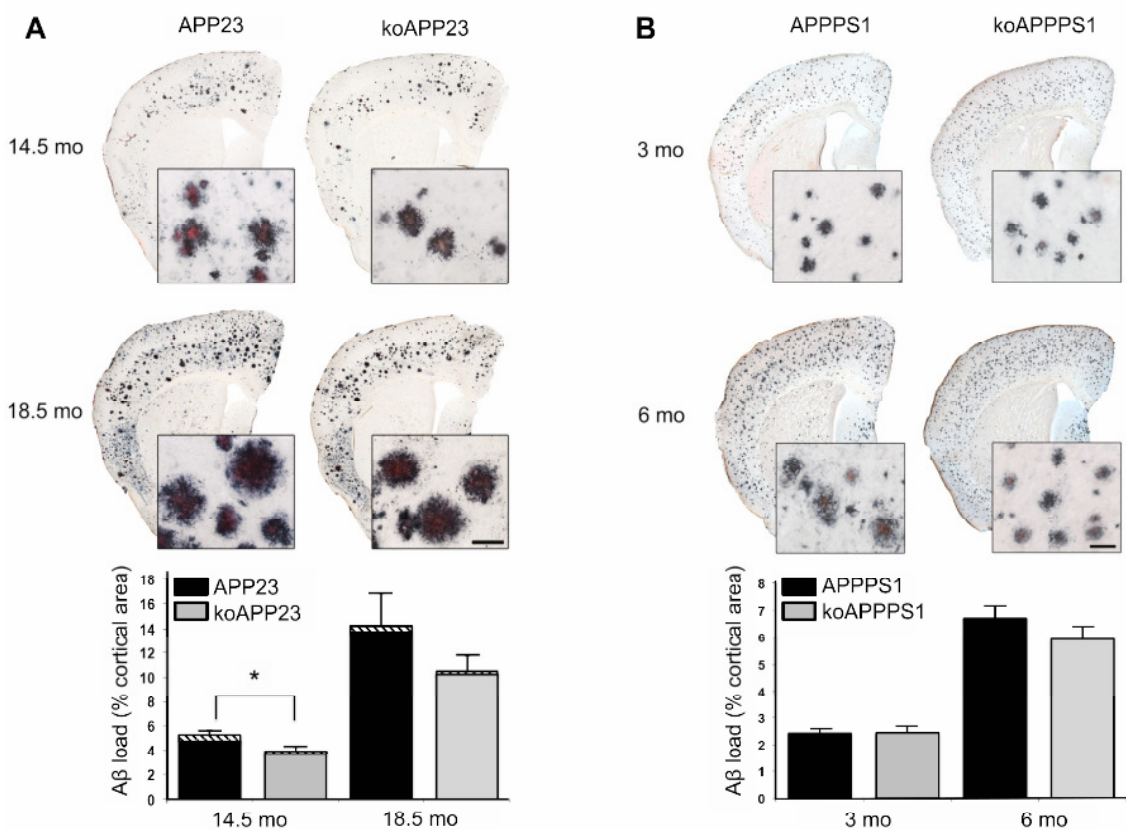
Figure 6. Aβ load in APP23 versus koAPP23 mice and APPPS1 versus koAPPPS1 mice. **(A)** Representative images of cortical brain sections from 14.5 and 18.5 month-old APP23 and koAPP23 mice stained with an antibody specific for Aβ (CN3) in combination with Congo red. Inserts represent higher magnification of cortical plaques. Stereological analysis of total Aβ load (CN3/Congo red-positive area as percentage of total cerebral cortex; 14.5 months: n=9 APP23, n=9 koAPP23, unpaired t-test, p=0.015; 18.5 month: n=4 APP23, n=6 koAPP23, unpaired t-test, p=0.19; error bars: SEM). The striped area at the top of the bars represents the percentage of vascular Aβ. **(B)** Representative images of cortical brain sections from 3 and 6 month-old APPPS1 and koAPPPS1 mice stained with CN3 and Congo red. Inserts represent higher magnification of cortical plaques. Stereological analysis of the Aβ load (CN3/Congo red-positive

area as percentage of total cerebral cortex area; 3 months: n=8 APPPS1, n=7 koAPPPS1, unpaired t-test, p=0.97; 6 months: n=8 APPPS1, n=6 koAPPPS1, unpaired t-test, p=0.44; error bars: SEM). The very minor amount of vascular amyloid in APPPS1 mice is not visible in the respective graphs. Scale bar: 50 µm for (A) and (B).

The accumulation of murine Aβ in both APP23 and APPPS1 mice prompted us to investigate whether murine Aβ is co-deposited with human Aβ in β-amyloid plaques. Brain sections were stained with the murine Aβ-specific antibody m3.2 and the LCO pFTAA. The m3.2 immunoreactivity closely matched pFTAA staining in both APP tg lines (Figure 7). No labeling for the m3.2 antibody was detected in brains of koAPP23 and koAPPPS1 mice. Both dyes showed labeling of the core and peripheral regions of the Aβ plaques in each mouse line.
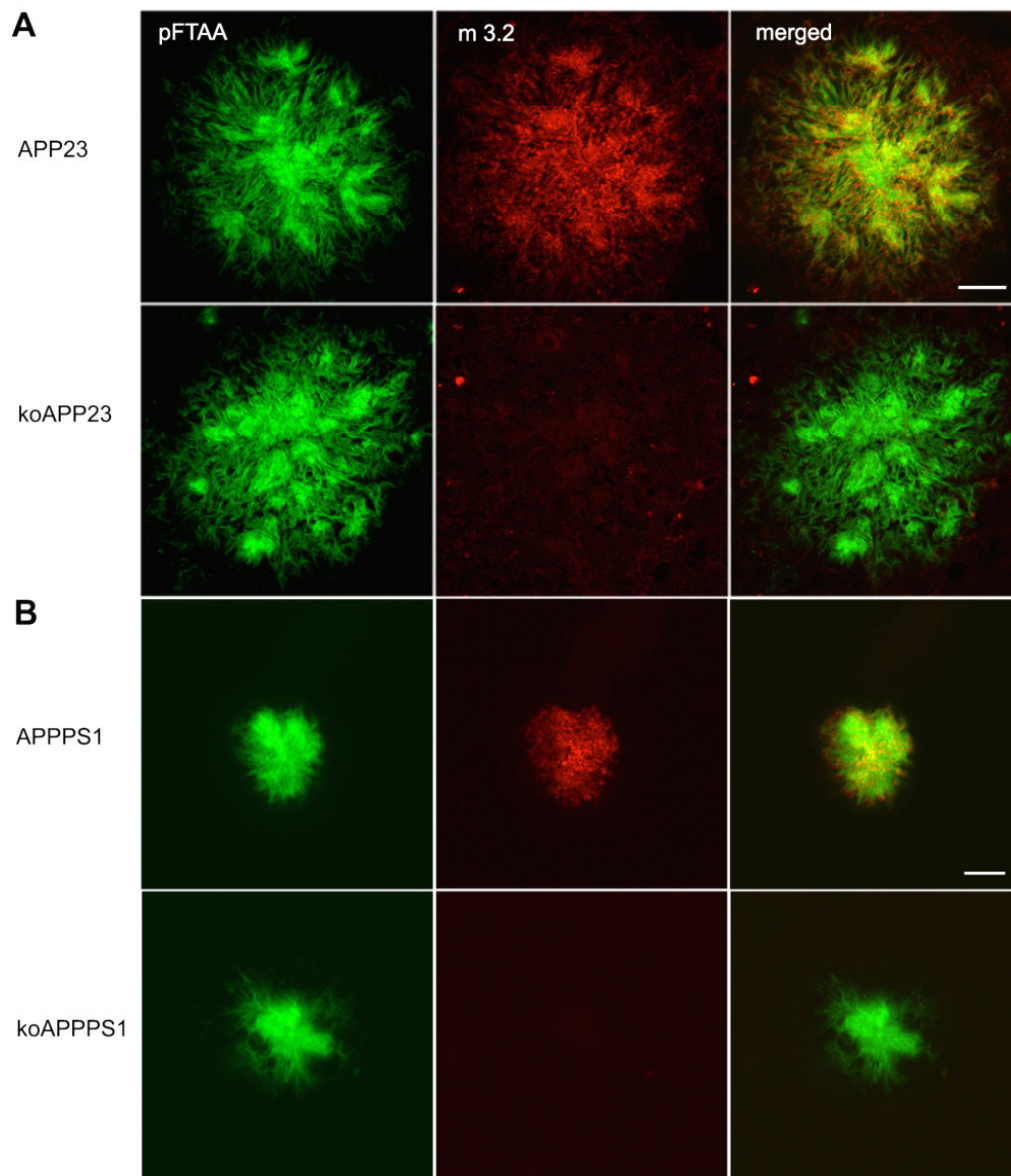
Figure 7. Murine Aβ is part of Aβ plaques in APP23 and APPPS1 mice. Immunohistological staining for murine Aβ (m3.2 antibody) is visible in Aβ plaques of 14.5 month-old APP23 **(A)** and 3 month-old APPPS1 **(B)** mice. Plaques were counter-stained with the amyloid-specific fluorescent dye pFTAA. As expected, no staining of murine Aβ was observed in koAPP23 and koAPPPS1 mice. Two representative animals were examined for each group (4 brain sections/animal). Scale bars: 20 µm for (A) and 10 µm for (B). Images in (B) represent maximum intensity projections of six z-planes each.

As murine and human Aβ deposit in close proximity in the plaques of the APP tg models that were investigated, we speculated that this tight association might result in different conformations of human versus mixed Aβ fibrils. In an initial attempt to identify such structural changes, 3-month-old APPPS1 and koAPPPS1 brain sections were stained with pFTAA and spectrally analyzed. For this analysis, APPPS1 mice were used, which depicted a high percentage

of co-deposited murine Aβ (data not shown; Mahler et al., 2015). pFTAA was previously shown to detect different plaque morphotypes (Lord et al., 2011) and was therefore used to investigate potential conformational differences in this study. Although, a slight tendency towards red-shifted wavelengths of the plaques with solely human Aβ could be observed, the spectral analysis was unable to detect significant differences between human and mixed mouse-human fibrils (Figure 8).
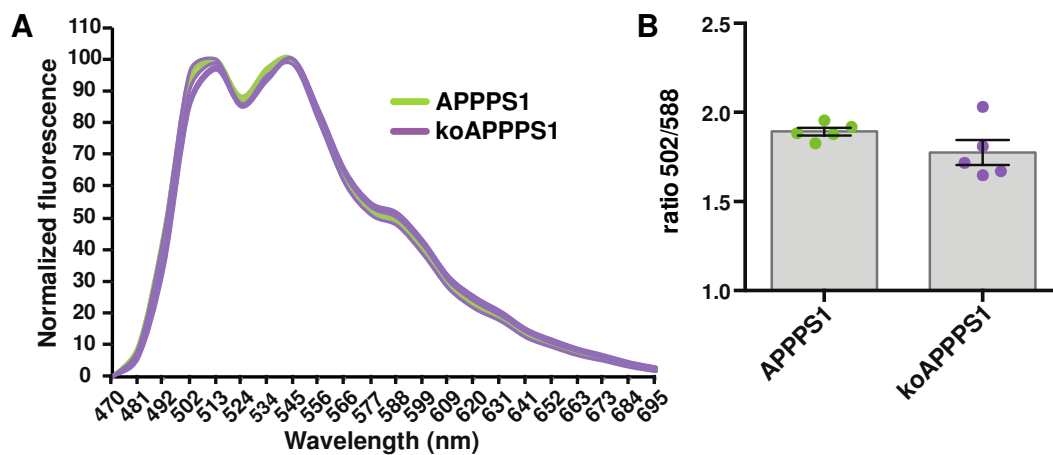
Figure 8. Spectral similarities between plaques of APPPS1 and koAPPPS1 mice. **(A)** Normalized emission spectra of APPPS1 (green) and koAPPPS1 (purple) mouse plaques, stained with pFTAA. Each curve represents the mean plaque spectrum per animal (n=14-16 plaques/animal). **(B)** For quantitative analyses the ratio of emitted light at 502 and 588 nm was assessed for individual Aβ plaques and the mean ratio determined per animal. Five animals were analyzed per line; 14-16 Aβ plaques per animal were considered. One dot represents one animal; data are mean ± SEM. Unpaired t-test revealed no significant differences between the two mouse lines (p=0.1465).

1.2. Different Aβ conformers in organotypic slice cultures

This section summarizes results from the published manuscript (Novotny, Langer*, Mahler et al., 2016).*

As exemplified by PrP, amyloid peptides harboring the exact same amino acid sequence can exhibit distinct, strain-like properties (Prusiner, 1998). This is also suggested for the Aβ peptide, which depicted differences in plaque morphology and LCO spectral properties in APP23 and APPPS1 mice, even after inoculation into host mice (Heilbronner et al., 2013). These conformational differences were now analyzed in hippocampal slice cultures (HSC), a novel model system combining the advantages of *in vitro* and *in vivo* approaches to study β-amyloidosis. In order for Aβ deposition to be triggered in slice cultures, one-time application of amyloid-laden extract from tg mouse brains and synthetic Aβ supplementation into the culture medium is required. Consequently, one could assume that Aβ aggregation in culture occurs via a seeded conversion mechanism.

To confirm such a mechanism, we analyzed the conformational characteristics of Aβ deposits in HSCs. Therefore, the HSCs were treated with brain extracts from either aged APP23 or APPPS1 mice and were incubated with medium supplemented either with synthetic Aβ1-40 (Aβ40) or Aβ1-42 (Aβ42). HSCs treated with APP23 brain extract and Aβ40 showed predominately large plaques whereas HSCs treated with APPPS1 extract and synthetic Aβ42 depicted rather small, compact plaques that were also more abundant (Figure 9A,D). Both the brain extract as well as the synthetic Aβ seemed to have an effect on the morphology of the induced deposits, as cultures treated with the combinations of APP23 extract/synthetic Aβ42 and APPPS1 extract/synthetic Aβ40 showed a mixed appearance (Figure 9B,C). This observation was confirmed with a spectral analysis of the different deposits. Sectioned HSCs from all treatment groups were stained with the LCO pFTAA, which revealed spectral differences between the deposits that can be attributed to distinct conformations (Figure 9E). The cultures treated

with the combination of APP23 extract/synthetic Aβ40 and APPPS1 extract/ Aβ42 exhibited the largest spectral differences, whereas the mixed treatment groups showed intermediate spectral properties (Figure 9E). Consequently, the origin of the applied seeding extract (APP23 or APPPS1) as well as the type of synthetic Aβ (Aβ40 or Aβ42) that was added into the culture medium had a significant influence on the induced plaque conformation.
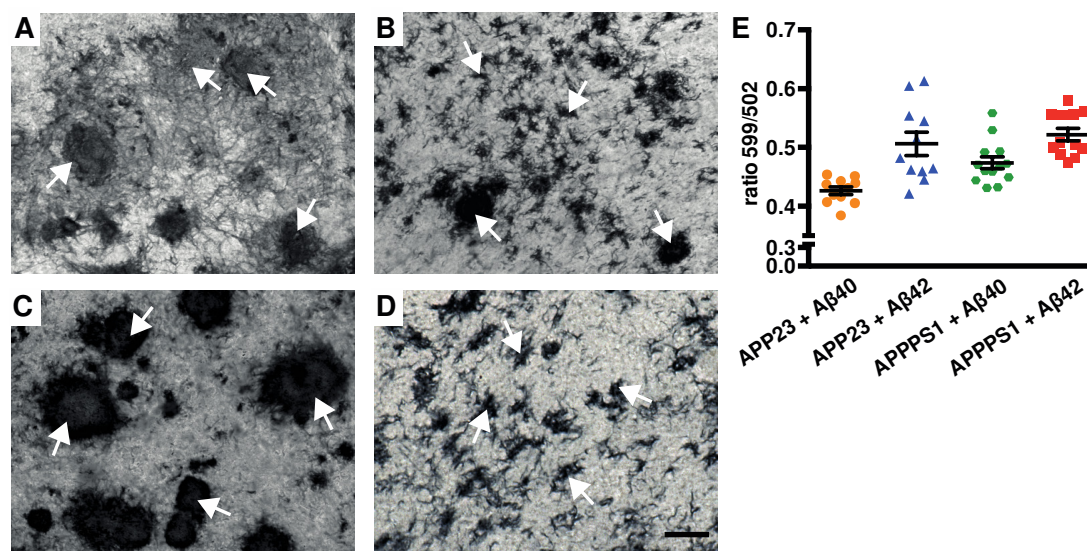
Figure 9. Aβ conformation in HSC's depends on the seed and synthetic Aβ species. **(A–D)** Differences in structural appearance of induced Aβ deposits (anti-Aβ immunostaining) in 10-week-old wt HSC's inoculated with different brain extracts and incubated with 1.5 µM of either synthetic Aβ40 or Aβ42 in the culture medium. **(A)** Large fibrillary deposits of Aβ (arrows) were observed with APP23 brain extract and synthetic Aβ40. **(B)** Inoculation with APP23 brain extract and synthetic Aβ42 revealed a mixed pattern of small and large fibrillary deposits. **(C)** APPPS1 brain extract combined with synthetic Aβ40 revealed large and compact deposits, whereas **(D)** numerous small deposits (arrows) were seen with APPPS1 brain extract and synthetic Aβ42. Scale bar: 20 µm. **(E)** Spectral properties of the induced Aβ deposits using the conformation-sensitive LCO pFTAA. For quantitative comparison, the ratio of light emitted at 599 and 502 nm was assessed for individual Aβ deposits and the mean ratio determined per HSC. 11–13 cultures per treatment condition were analyses and each 4–15 Aβ plaques. One dot represents one culture; data are mean ± SEM. ANOVA (extract × synthetic Aβ) revealed a significant effect for extract ($F_{(1,43)}$=6.41; $p<0.05$) and synthetic Aβ ($F_{(1,43)}$=26.17; $p<0.001$) but failed to reach significance for the interaction ($F_{(1,43)}$=1.61; $p>0.05$).

1.3. Aβ conformers are preserved after formaldehyde fixation

This section summarizes results from the published manuscript (Fritschi, Cintron*, Ye, Mahler et al., 2014).*

Aβ seeds bear many similarities to classical prions illustrated by their potential to induce Aβ aggregation in the living brain by the inoculation of exogenous seeds (Walker et al., 2002, Meyer-Luehmann et al., 2006, Eisele et al., 2009, Eisele et al., 2010, Langer et al., 2011) and their strain-like behavior while transmitting different Aβ conformations to the next generation (Heilbronner et al., 2013). Moreover, prions are remarkable for their resistance to inactivation by formaldehyde. In this study, it was shown that Aβ seeds also resemble prions in this regard by retaining their ability to induce Aβ deposition in tg mice even after the donor tissue has spent years in formaldehyde. Consequently, we investigated whether different Aβ conformers could also be preserved, following formaldehyde fixation.

Extracts from fixed and fresh-frozen APPPS1 and APP23 hemispheres were intracerebrally injected into young APP23 tg mice and immunohistochemically analyzed after 4 months. The morphology of the Aβ deposits looked typical for the respective mouse line when mice were injected with the fresh-frozen brain extracts (i.e. large Aβ plaques with diffuse periphery for APP23 mice, and small, compact deposits for APPPS1 mice; Figure 10A,B). However, fixed donor extracts from both APP23 and APPPS1 tg mice gave rise to Aβ plaques that were rather small and compact (Figure 10C,D). Subsequent spectral analysis revealed that the LCO pFTAA is able to spectrally discriminate between Aβ deposits in mice that were injected either with fresh-frozen APP23 or fresh-frozen APPPS1 brain extract (Figure 10E). The spectral analysis of plaques induced by the injection of fixed APP23 or fixed APPPS1 brain extracts showed as well a significant difference (Figure 10E), similar to that in unfixed tissue. In summary, pFTAA is still able to detect different Aβ conformations between APP23 and APPPS1 mice after formaldehyde treatment.
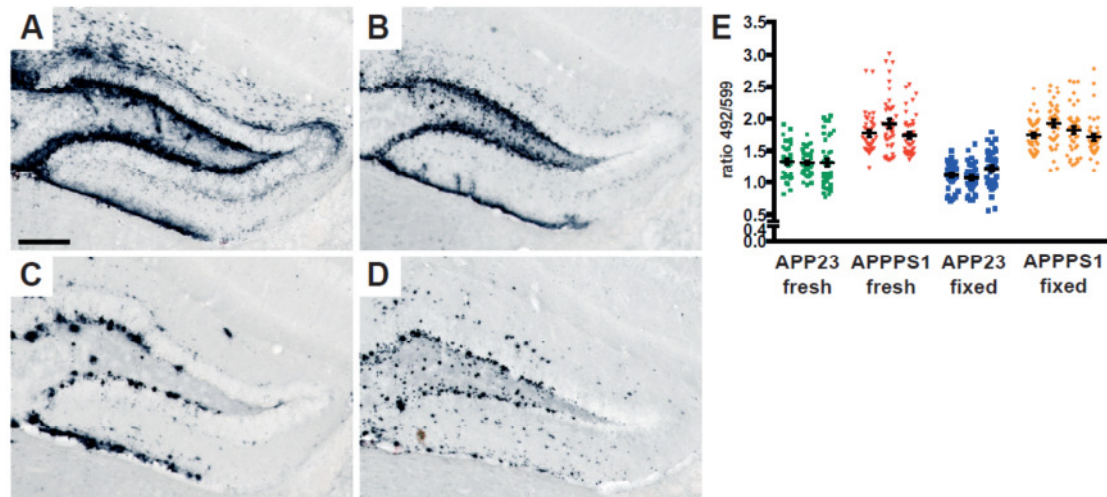
Figure 10. Formaldehyde fixation preserves strain-like properties of seeded Aβ plaques. Brain extracts from aged APPPS1 or APP23 tg donor mice were intracerebrally injected into pre-depositing, 3–4 month-old APP23 tg host mice. Brains were analyzed 4 months after inoculation using Aβ immunostaining. **(A-D)** The extract of the fresh-frozen APP23 brain tissue induced a more diffuse pattern of Aβ deposition **(A)**, whereas the extract of the fresh-frozen APPPS1 brain tissue induced a more punctate pattern **(B)**. Injection of extracts from formaldehyde-fixed brain tissue induced a more punctate pattern for both APP23 **(C)** and APPPS1 **(D)** donor mice. Scale bar: 200 μm. **(E)** Spectral properties of the induced Aβ deposits using the LCO pFTAA. For quantitative analysis, the ratio of the intensity of the emitted light at 492 and 599 nm was calculated. Each dot represents one Aβ plaque. The mean and SEM are indicated for each animal (n=3–4/group). ANOVA (genotype of donor material × tissue preparation) revealed a significant effect of the donor genotype ($F_{(1,9)}=165.6$; $p<0.001$) but no significant effect of the tissue preparation ($F_{(1,9)}=4.856$; $p=0.055$) or interaction ($F_{(1,9)}=3.947$; $p=0.078$).

2. Aβ conformers in Alzheimer's disease patients

In a recent study, differences in the Aβ fibril structure were identified between two AD patients (Lu et al., 2013). A single predominant Aβ fibril structure was detected in each case, suggesting that fibrils in the brain may spread from a single nucleation site. In a separate study, came indications that a special subtype of AD, termed rapid AD given the expedited cognitive decline in these patients, contain different Aβ structures as shown by detergent insolubility and aggregate sizes (Cohen et al., 2015). Consequently, variations in AD may arise from distinct Aβ fibril structures. Indeed, many factors might contribute to the phenotypic appearance of the disease and the impact of different structural characteristics and their relation to the clinical phenotype remains obscure for the broader population of AD patients. In this study, we aimed to expand our understanding of structural variations in plaques of different AD cases. To achieve this goal we performed spectral analysis of AD tissues stained with the conformation-sensitive dyes described before.

2.1. Morphological characterization of Alzheimer's disease plaques

The plaque morphology was investigated in eight FAD cases (with an APP V717I, PSEN1 A431E or PSEN1 F105L mutation; see Table 2) and 18 SAD cases by fluorescent microscopy. Fresh frozen brain sections were stained with the LCOs qFTAA and hFTAA in order to spectrally characterize all ultra-structural components of the amyloid deposits (Nystrom et al., 2013). In all cases compact Aβ plaques and diffuse Aβ deposits could be observed (Figure 11). The number of deposits and the proportion of compact versus diffuse plaques varied slightly between particular sections and regions, however a rather homogenous picture of deposition was observed looking at the overall set of AD patients. A single exception constituted a SAD case previously described to exhibit a significantly reduced high-affinity binding of PIB (PIB[neg]) (Rosen et al., 2010). The plaque morphology proved special in this case, depicting a faintly stained plaque core surrounded by an area with strong staining resulting in a "ring-shaped" appearance of these plaques. What was described for 6E10-immunostained plaques in Rosen *et al.* (2010) could be confirmed with qFTAA/hFTAA staining in this study (Figure 11). Ring-shaped compact as well as more diffuse Aβ plaques were seen in this case. Diffuse

deposits as predominantly seen in all other AD cases were rather rare in this case with deficient PIB binding.
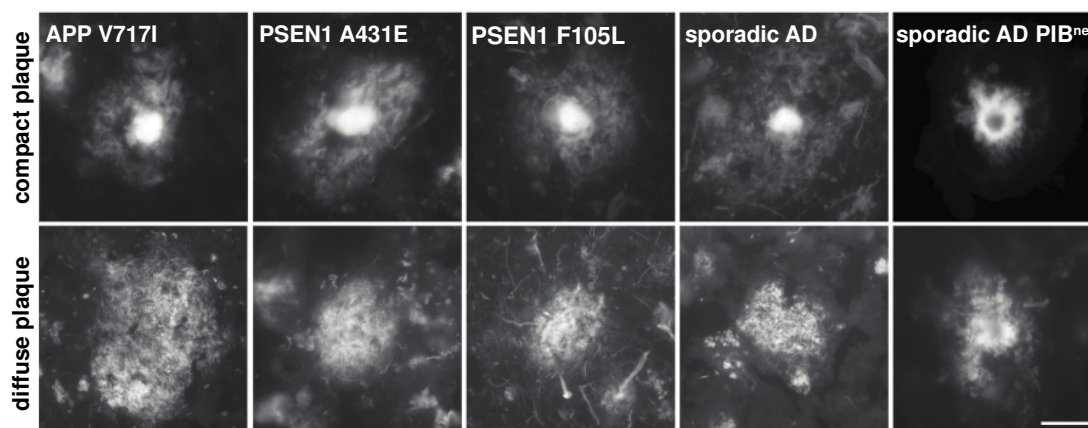
Figure 11. Plaque morphologies of sporadic and familial AD cases. Representative images of qFTAA and hFTAA stained compact (upper row) and diffuse (lower row) Aβ plaques in the frontal cortex. In general, plaques from sporadic AD cases are morphologically similar to plaques from familial cases (APP V717I, PSEN A431E and PSEN F105L mutations). Only the PIB[neg] sporadic AD case showed a specific, distinct plaque morphology. In comparison to the other AD cases, the PIB[neg] case exhibited a weaker qFTAA/hFTAA staining in the plaque core, for compact (upper row) as well as diffuse (lower row) Aβ plaques. Scale bar: 20 μm.

2.2. Biochemical analysis of Alzheimer's disease tissue

The tissue samples from all AD patients were analyzed for their Aβ load and Aβ42/40 ratio *(experiments performed by Jay Rasmussen)*. Brain tissue homogenates were analyzed by an electro-chemiluminescence immunoassay (MesoScale Discovery). Looking at the Aβ amount, the PIB[neg] case occupied again a unique position, showing an extremely high Aβ load compared to all other cases (Figure 12A, red). Within the FAD cases, the PSEN1 A431E mutation cases (blue) showed a slightly higher Aβ load than the PSEN1 F105L (grey) cases and the APP mutation (green). The SAD cases (orange) seemed to have an overall lower Aβ load than the PSEN1 A431E cases, with the exception of the PIB[neg] case and one other SAD case (AD13). The Aβ42/40 ratio was highest in the APP mutation cases and also generally high in the SAD cases, again with the exception of the PIB[neg] case and AD13, whose high Aβ load seemed to mainly arise from high Aβ40 (Figure 12B).
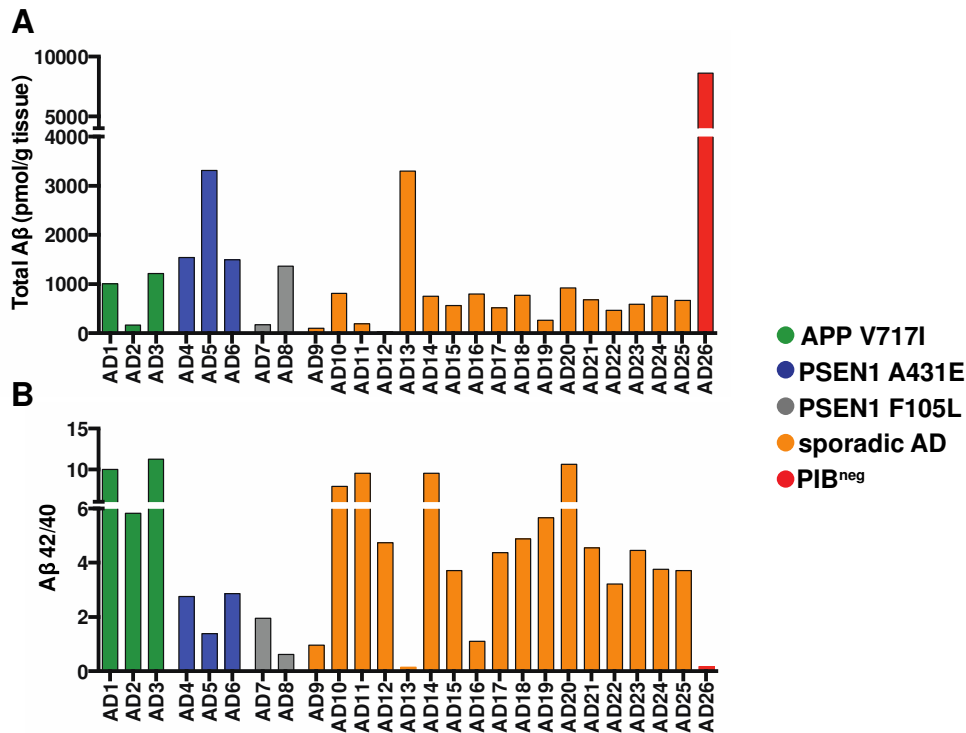
Figure 12. Biochemical characterization of AD brain tissue (*performed by Jay Rasmussen*). **(A)** Total Aβ load in pmol/g tissue from all FAD and SAD cases measured by MesoScale after formid acid extraction. The different groups are indicated in the legend. **(B)** Aβ42/40 ratio calculated from total Aβ40 and Aβ42 values for all patients.

2.3. Different Aβ conformers among human amyloid plaques

Seeing as the PIB[neg] case showed a unique plaque morphology and different biochemical characteristics in addition to the drastically reduced PIB binding, one could assume that this case also harbors a special distinct plaque conformation. Consequently, the PIB[neg] case was foremost compared for conformational differences against six other SAD cases in order to confirm that the spectral analysis method we have applied so far to reveal fine plaque structural detail can pick up any differences in the internal plaque organization. Thus, qFTAA/hFTAA stained sections were examined; staining revealed a prominent difference between the PIB[neg] case and the SAD cases, both visually perceivable and quantifiable by spectral analysis (Figure 13A,B).
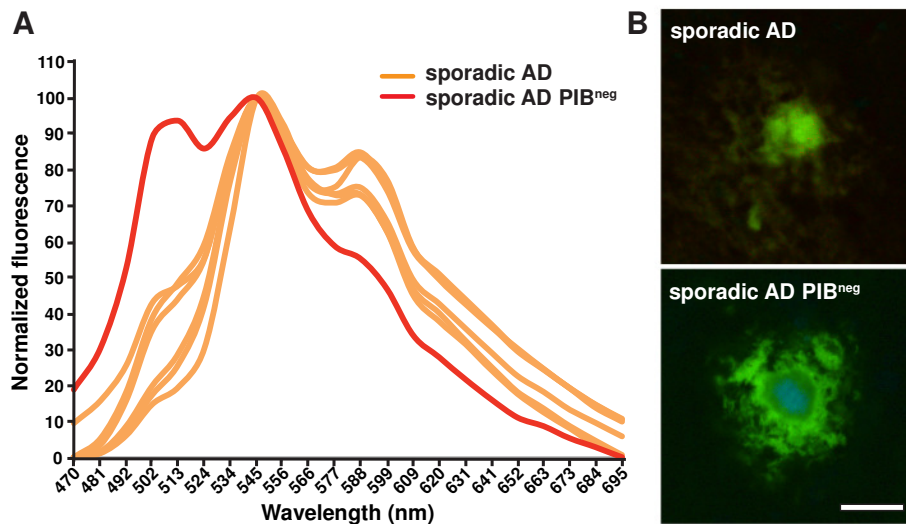
Figure 13. The PIB[neg] case shows a distinct spectral signature. **(A)** Normalized spectral curves of sporadic AD patients showing that the PIB[neg] case (red) has a blue-shifted spectrum compared to six other sporadic AD cases (orange). Each curve represents the mean plaque spectrum from one patient (n=45-60 plaques/patient). **(B)** Images of plaques in a sporadic AD case and the PiB[neg] case. Colors are created from spectral color-coding of the acquired images. The distinct blue-shifted core of the PiB[neg] plaques is clearly distinguishable on the sections. Scale bar: 20 µm.

Following these experiments where the plaque structure of a unique AD case stood out from the structures of regular SAD cases, plaques of all SAD and FAD cases were considered to discern inter-group differences. To visualize the spectral differences between single plaques the ratio of emitted light was calculated from the regions with maximal spectral separation, at 502 nm and 588 nm respectively. The ratios of the qFTAA/hFTAA stained sections revealed significant differences between FAD and SAD cases. For the FAD cases, the plaque spectra of the single patients looked quite similar to each other within any of the three mutations (Figure 14A,B). However, between the mutations differences could be detected. Looking at the means of the three PSEN1 A431E mutation cases, these were significantly different from all other FAD and the SAD cases (Figure 14B). In addition, the APP mutation cases were significantly different from the SAD; only the PSEN1 F105L mutation cases were quite similar to the APP mutation and SAD cases. Looking at the single plaques measured for each patient a certain spectral variability was observed, indicating that even in individual patients, plaques can exhibit quite diverse structural characteristics (Figure 14A).
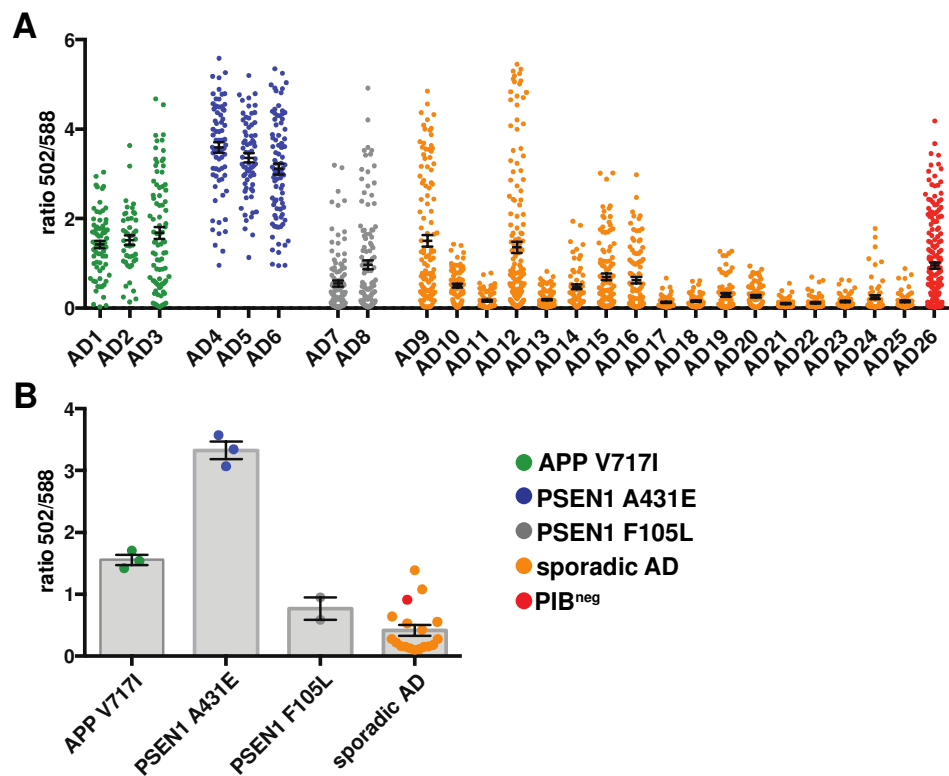
Figure 14. Conformational differences between FAD and SAD cases. **(A)** qFTAA and hFTAA stained brain sections from all FAD and SAD cases were spectrally analyzed and the ratio of emitted light at 502 nm and 588 nm was calculated to quantify the spectral differences. 45-190 plaques were analyzed per patient. One dot represents one plaque and mean ± SEM is indicated for each patient. **(B)** For statistical analysis the mean was calculated for the different mutations groups and SAD (including PIB[neg]) from the means of the single patients. One dot represents one patient and mean ± SEM is indicated per group. ANOVA revealed significant differences between the groups (n=26, 2-18/group; $F_{(3,22)}$=64.88; $p<0.0001$). Bonferroni post-hoc analyses were applied for multiple comparisons with the statistical significance set at $p<0.05$. PSEN1 A431E cases were significantly different from APP V717I, PSEN1 F105L and SAD ($p<0.0001$). APP V717I was significantly different from SAD ($p<0.001$). PSEN1 F105L was not different from APP V717I and SAD ($p>0.05$).

Next, we wanted to assess the intra-individual variation in spectral signatures. Therefore, we analyzed differences among three different neocortical regions in each of the groups: the superior middle temporal gyrus (SMTG), the middle frontal gyrus (MFG) and the pericalcarine region of the occipital lobe (OL). For the FAD cases small differences were observed between the three regions, although the spectra appeared all together similar for the different mutation groups (Figure 15A). In the sporadic cohort, some cases showed greater differences among regions (e.g., AD9 and AD12, Figure 15B), but in general the spectral signatures were fairly homogeneous in a given individual. For all cases, we did not observe that a single brain region was consistently different from the other regions. However, in the two SAD cases that appeared as

outliers (AD9 and AD12) it seemed that the SMTG spectra was quite blue-shifted.
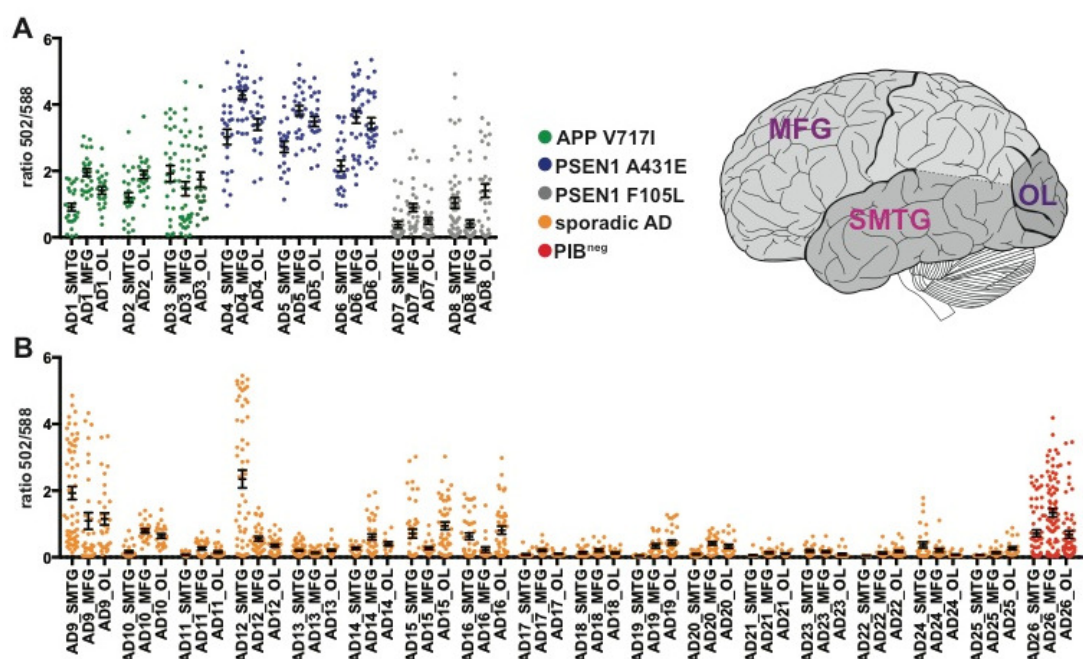
Figure 15. Different brain regions show predominantly spectral similarities. **(A,B)** Ratio of emitted light at 502 nm and 588 nm was calculated for quantitative comparison of individual Aβ plaques. 18-76 plaques were analyzed per region, for the SMTG, the MFG and the OL of all FAD **(A)** and SAD **(B)** cases. One dot represents one plaque; mean ± SEM are indicated for each region.

2.4. Conformational differences are not directly attributable to a single disease-associated characteristic

The structural heterogeneity observed for the different mutations of FAD cases might be partly attributable to the genetic, biochemical and phenotypic differences described previously (Larner and Doran, 2006, Maarouf et al., 2008, Ringman et al., 2014, Roeber et al., 2015). More intriguing were the conformational differences seen within the group of SAD cases representing the vast majority of affected patients, for which the origin of the observed heterogeneity is mainly obscure. Therefore, we wanted to confirm that the observed spectral differences are not associated with factors that might influence the plaque conformations such as the age of the patients, the post-mortem interval (PMI), biochemical characteristics and the ApoE genotype. The mean LCO ratio for each SAD patient was hence correlated with the

respective factor (Figure 16A-D) and for ApoE the LCO ratios were compared for the different genotypes (Figure 16E). None of the factors showed a correlation with the LCO ratio and distinct ApoE genotypes depicted similar spectral properties.
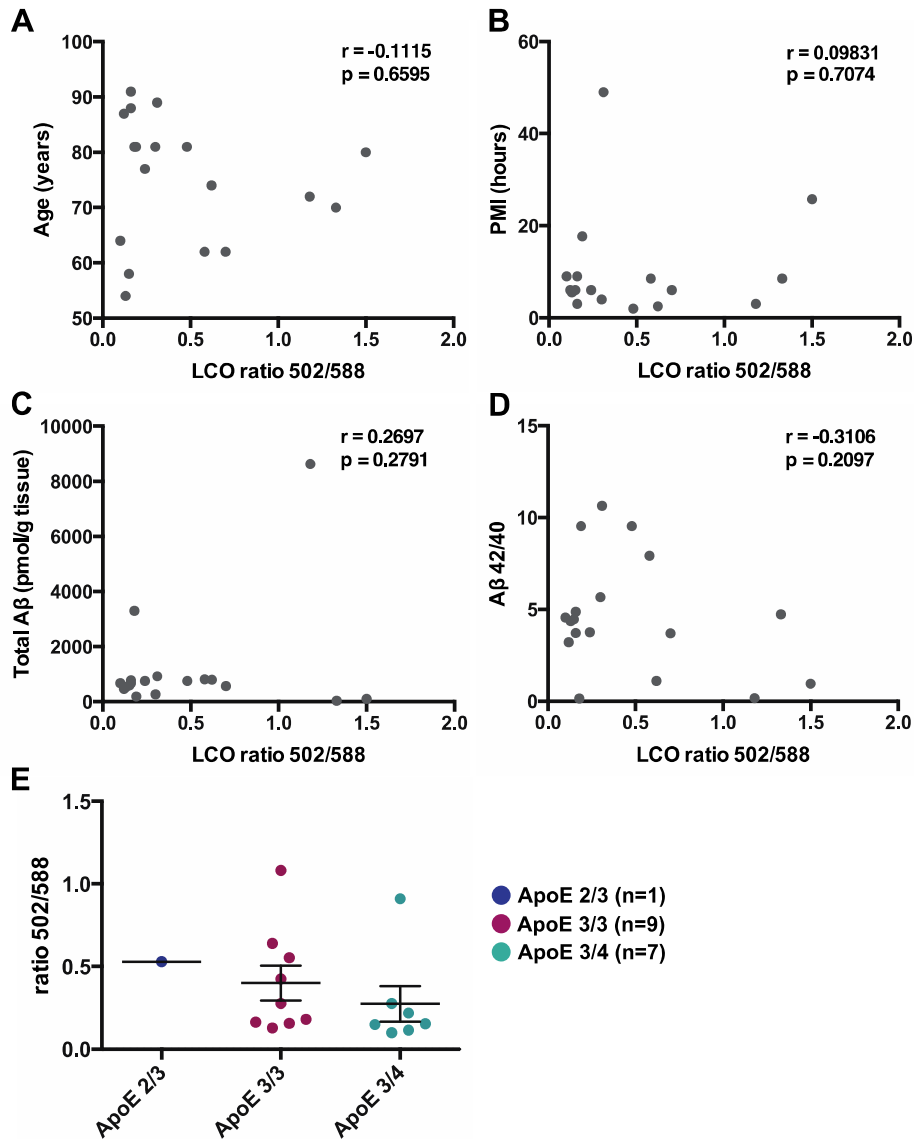
Figure 16. Disease-associated factors are not responsible for distinct LCO ratios. **(A-E)** Correlations between age **(A)**, PMI **(B)**, total Aβ load **(C)**, Aβ42/40 **(D)** ratio and the LCO ratio 502/588 nm of the respective SAD patients. Pearson's correlation coefficient r and its p-value indicate that none of the correlations were statistically significant. **(E)** SAD patients (n=17; for AD9 the ApoE genotype was not available) were divided into three groups according to their ApoE genotype as indicated in the legend. One dot represents one patient. Mann Whitney test revealed no difference between the ApoE3/3 and ApoE3/4 genotype (p=0.2061).

In summary, spectral imaging of the qFTAA and hFTAA double-stained human AD tissues revealed variations between plaques of certain FAD and SAD cases and most interestingly detected a conformational heterogeneity within SAD patients that is not directly correlated to a certain disease-associated characteristic.

Discussion and Conclusions

Although much has been discovered about the molecular processes underlying AD pathology in the past years, major questions have not been answered and a cure for this pervasive malady is elusive. The Aβ peptide, one of the principle aggregating proteins in AD and a target for therapeutics, is presented with a structural heterogeneity reminiscent of prion strains. The strain-properties of Aβ aggregates have been structurally analyzed in this thesis in different models of β-amyloidosis and human post-mortem brain tissue. A detailed knowledge about the structural differences of amyloid proteins would be essential to understand the biological effects arising from structural variations (Tycko, 2015). Ultimately, the goal is to use this knowledge for the development of new compounds that bind to specific kinds of pathogenic amyloid fibril structures, both for diagnostic imaging (Klunk et al., 2004) and/or for inhibiting aggregation (Estrada and Soto, 2007).

Aβ conformers in models of β-amyloidosis

Mouse models, developed on the basis of the familial disease mutations, recapitulate many aspects of the disease, hence they are suitable tools to analyze the hitherto unexplored molecular processes. Most human APP tg mouse models of AD generate endogenous murine Aβ together with tg human Aβ. Yet the role of the murine peptide in amyloid formation is not well understood. Murine Aβ differs from human Aβ in its amino acid sequence and might potentially also show dissimilarities in the conformation. In this regard, the influence of murine Aβ on the amyloidosis in mouse models remains ambiguous. As a first step in our study, we addressed whether murine Aβ has an influence on the amyloid deposition in different mouse lines. Accordingly, the amyloid load was assessed by stereological analysis in APP23 and APPPS1 mice. We saw a significant increase of cerebral β-amyloid load in 14.5 month-old and 18.5 month-old APP23 mice compared to koAPP23 mice lacking endogenous mouse APP and Aβ. At both ages, parenchymal plaques and CAA were elevated with an even stronger increase of the rather rarely found CAA. Interestingly, the amyloid load did not differ significantly between

APPPS1 and koAPPPS1 mice, in contrast to the striking difference observed in APP23 mice. In a previous study, mouse APP has been overexpressed in APPswe/PS1dE9 mice with the amyloidosis burden being intermediate between APP23 and APPPS1. This resulted solely in an increase in CAA but not in faster or more extensive plaque deposition (Jankowsky et al., 2007).

Seeing an impact on the amyloid load, we next investigated whether human and murine Aβ are co-deposited in plaques of APP23 and APPPS1 mice. Staining with the murine-specific antibody m3.2 and the conformation-sensitive dye pFTAA revealed murine Aβ in tight association with human Aβ in amyloid fibrils. This result was confirmed by electron microscopy (Mahler et al., 2015) and is in line with studies suggesting the formation of mixed human-murine fibrils *in vitro* (Fung et al., 2004) and the co-deposition (Pype et al., 2003, van Groen et al., 2006a) or co-immunoprecipitation (Morales-Corraliza et al., 2013) of murine and human Aβ within the mouse brain. The tight association of human and murine Aβ in amyloid fibrils could result in conformational differences compared to fibrils composed of purely human Aβ. In order to investigate potential structural differences, the fluorescence emission of the LCO dye pFTAA, bound to human and mixed human-mouse amyloid fibrils, was spectrally investigated. We decided to analyze APPPS1 mice for this purpose, because they showed the highest percentage of murine Aβ (Mahler et al., 2015). Even though a small tendency towards red-shifted spectra of the koAPPPS1 mice could be detected, no significant spectral differences were observed between APPPS1 and koAPPPS1 plaques. However, very fine differences below the detection limit of the herein tested dye could exist. Future experiments to assess a structural influence of murine Aβ should also include the APP23 and koAPP23 mice with increased animal numbers. Therefore, final conclusions about conformational differences between the Aβ subtypes cannot be drawn until further analyses have been performed. However, these data indicate that the structural micro-organization within the plaque is similar in mice with or without the murine subtype. Intriguingly, this similarity was observed despite the contribution of different materials to the build-up of the plaque, which is in line with studies suggesting

seeded templating (reviewed in Jucker and Walker, 2013, Walker and Jucker, 2015). Consequently, the overproduced human Aβ subtype may predominately influence the plaque conformation, with material diversity contributing a minute effect, in the mice with both subtypes. Taken together, our data show that the impact of mouse Aβ on amyloidosis differs among APP tg mice and seems to decrease in more aggressive models. Mouse Aβ may therefore affect study outcomes differently depending on the model used and should thus be addressed in individual lines, before reaching conclusions based on the modeled humanized β-amyloidosis.

Another set of experiments should address whether Aβ conformers and the concept of seeded templating are dependent on the biological system. To this end, we tested conformational differences of Aβ in an organotypic slice culture model, using mouse HSCs and a combined treatment approach with Aβ seeding extract and synthetic Aβ. It was first shown for prions that differences can exist between the conformations of the proteins even though the underlying amino acid sequence is exactly the same (Pan et al., 1993, Bessen and Marsh, 1994, Prusiner, 1998). This behavior was recently confirmed for the Aβ peptide. Different Aβ conformers were shown to exhibit distinct biological activities *in vitro* (Petkova et al., 2005, Eisenberg and Jucker, 2012) and polymorphic Aβ deposits as well as structural Aβ variants have been described in APP tg mouse models (Heilbronner et al., 2013) and AD brains (Lu et al., 2013). In our study we demonstrated that also in HSCs Aβ conformers could be observed and that plaque formation occurs, as in prion diseases, via a templated conversion mechanism (Novotny et al., 2016). Spectral analysis of Aβ deposits stained with the conformation-sensitive dye pFTAA revealed different Aβ morphotypes. These differences proved dependent on the nature of the synthetic Aβ species in the culture medium (Aβ40 versus Aβ42) and also on the applied brain extract (APP23 or APPPS1 mice). The combined treatment of APP23 extract and synthetic Aβ40 gave rise to large, diffuse plaques with a red-shifted spectral signature, which underscores the more diffuse Aβ arrangement in these deposits. Treatment with APPPS1 extract and synthetic Aβ42 induced rather small, compact plaques with a blue-shifted spectrum supporting the more dense Aβ

arrangement in these deposits. In agreement with this, the cross-treatments (APP23/Aβ42 and APPPS1/Aβ40) generated Aβ plaques with mixed morphology and intermediate spectral properties, showing that both the applied seeding extract and the synthetic Aβ contribute to the amyloid formation. Of note, the amyloid-associated changes in HSCs occur in wt brain tissue thus avoiding the potential confounding overexpression of APP in tg mice (Jucker, 2010). Seeded Aβ aggregation in HSCs is a unique and valid model of β-amyloidosis, also for SAD. Systems that model the complex brain environment are urgently needed to study the mechanisms governing Aβ aggregation *in vivo* and to test therapeutic approaches (Forman et al., 2004). Our data demonstrate that different Aβ conformers can be found in HSCs and therefore seem to be independent of the biological system. In conclusion, our study provides evidence that conformational differences and strain-like behavior can be successfully studied in this rapid and easy accessible novel model system.

We further investigated Aβ conformers in mouse models of β-amyloidosis, this time with a focus on the exceptional durability of prion-like proteins. The persistent infectivity of prions even after exposure to formaldehyde for month or years (Pattison, 1965, 1972, Brown et al., 1986) was one of the earliest indications that the causative agent of Scrapie was unlike conventional infectious agents (Pattison, 1965). In our study, it was shown that Aβ seeds, like prions, are resistant to inactivation by formaldehyde (Fritschi et al., 2014). We demonstrated that apart from their amyloid-inducing activity, the conformational differences between Aβ aggregates are also maintained in formaldehyde fixed tissue. In accordance with previous studies (Heilbronner et al., 2013), we found morphological and conformational differences between plaques induced from brain extracts of fresh-frozen APP23 and APPPS1 mice. Remarkably, spectral analysis of pFTAA-stained sections still showed structural differences between APP23 and APPPS1 plaques, when mice were inoculated with fixed extracts. The morphology of the induced amyloid deposits was rather similar here. Consequently, formaldehyde fixation may partially modify the histological appearance of seeded Aβ plaque morphology, but at the same time maintain at least some of the basic conformational

properties of the aggregated Aβ. The present findings highlight the extraordinary robustness of Aβ seeds and in light of previous studies showing that Aβ seeds remain functional following boiling (Meyer-Luehmann et al., 2006) or drying (Eisele et al., 2009), our results further underscore their resemblance to prions. In summary, the formaldehyde-fixed Aβ seeds largely retained their conformational templating capacity, as the nascent amyloid deposits replicated the spectral properties of the parental seeds, at least at the binding-sites of the conformation-sensitive dye. Conclusively, the discovery that both the self-propagating activity and strain-like features of aggregated Aβ are maintained in fixed tissue supports their incorporation into the broad conceptual framework of prions.

In conclusion, the use of animal models to study amyloidosis *in vivo* and/or *ex vivo* has many advantages as the models often resemble the pathological lesions seen in patients remarkably well and at the same time constitute a fast-replicating system which can be easily manipulated. In this thesis we showed that mouse models and HSCs are even capable to recapitulate the different conformational characteristics of amyloid diseases. However, one should consider that the endogenous mouse Aβ could have an influence on the pathology in tg mouse models, an aspect which should be respectively noted and addressed. Moreover, regarding animal models used in translational studies, certain structural and/or biochemical variations may exist between the human and animal amyloids due to the different environment. This is exemplified by a difference in solubility between the human and mouse Aβ species (Kuo et al., 2001) or the low retention of PIB in mouse models compared to human AD brains (Klunk et al., 2005). In all nonhuman animals, Aβ deposits might be structurally different on a conformational level and this difference could be associated with the disease mechanism (Levine and Walker, 2010). In order to investigate variations in the structural level among human aggregates and disease cases, conformational differences were studied in plaque deposits of post-mortem human AD tissue.

Aβ conformers in Alzheimer's disease patients

Post-mortem brain tissues from 26 pathologically diagnosed AD patients were studied in terms of morphological, biochemical and conformational characteristics of their Aβ plaque pathology. FAD mutation cases harboring an APP (V717I) or PSEN1 (A431E or F105L) mutation, as well as SAD cases including one remarkable case of deficient PIB component binding, were analyzed. A distinct plaque conformation in the PIB[neg] SAD case was readily observed. Since this case was described to have a distinct plaque morphology and significantly elevated Aβ values in terms of total Aβ and Aβ40 (Rosen et al., 2010), which was confirmed in our study, we set off to investigate whether the structure of those plaques would also be unique. A well-defined LCO spectral blue-shift of the plaque cores was detected in this PIB[neg] case, so prominent that it could be visually distinguished as well (see Figure 13). This corroborated the fact that our qFTAA/hFTAA LCO pair is applicable and able to distinguish variable plaque conformations in human tissue. Consequently, we applied both LCOs to stain and analyze the entire AD cohort and uncovered remarkable differences between morphologically and biochemically similar Aβ plaques from FAD and SAD cases. The PSEN1 A431E mutation cases showed the biggest difference compared to both to the other FAD and the SAD cases. Plaque spectra from these patients were significantly blue-shifted compared to the other cases, indicating a higher percentage of qFTAA staining in these plaque cores, which might originate from a high proportion of mature Aβ fibrils and a compact fibril arrangement (Nilsson et al., 2007, Nystrom et al., 2013). The APP V717I mutation cases were still significantly blue-shifted from the SAD cases, albeit red-shifted compared to the PSEN1 A431E cases. Cases from the second PSEN1 mutation, F105L, were significantly red-shifted from the first PSEN1 mutation and rather similar to the APP mutation and SAD cases. This could indicate that patients with the F105L mutation in PSEN1 have a more diffuse Aβ arrangement in their plaques compared to the patients harboring the A431E mutation. This difference between the PSEN mutations was not completely unexpected, since a substantial phenotypic, histopathological and molecular heterogeneity is described for PSEN mutation cases (Larner and Doran,

2006, Maarouf et al., 2008, Roeber et al., 2015). In general, variations in the phenotypic and molecular characteristics are common among the familial forms. Interestingly, we found conformational differences also between the SAD patients, which support the idea that certain heterogeneity also exists between SAD cases (De Kimpe and Scheper, 2010, Janocko et al., 2012, Warren et al., 2012, Mattsson et al., 2016). It should be noted, however, that the heterogeneity between FAD cases with different mutations, which is supported by the high clinical symptom variability, may simply reflect the genetic, neuropathological and biochemical diversity in these patients. For SAD, the risk-genes can explain only about 30% of the phenotypic variations (Cohen et al., 2016) leaving the factors that lead to a heterogeneity in SAD largely elusive (Di Fede et al., 2013, Mattsson et al., 2016).

Amyloid deposition in the human brain is a progressive process that follows a distinct sequence, in which different brain regions are hierarchically affected (Braak and Braak, 1991, Thal et al., 2002, Thal et al., 2014). This concept hints to the possibility that differences in the amyloid conformation could be influenced by different plaque maturation stages in the respective brain region. Therefore, we spectrally investigated the plaque conformation in three different brain regions, for each patient. Spectra from SMTG, MFG and OL showed small variations for the FAD cases, but seemed overall quite similar within each group of the familial patients. The SAD cases were presented with a different pattern as more pronounced differences were detected in certain regions. In particular, the SMTG plaque spectra were showing a blue-shift in two of the SAD cases. Generally, the plaque pathology is thought to start in the neocortex, which includes all the brain regions investigated herein, and further spread into deeper brain areas (Braak and Braak, 1991). However, it is also known that for single patients the start and spreading of the Aβ pathology can vary substantially. Consequently, the blue-shift of the plaques in the SMTG, which hints to a more dense amyloid packing or a more maturated state of the fibrils compared to more reddish plaques, may arise from a different maturation stage in those regions. However, these differences may just as well be influenced by other, unexplored factors such as neuroinflammatory processes or yet undefined co-factors.

Lately, the paradigm from Braak *et al.* (1991) has been refined describing distinct biochemical stages of amyloid deposition and their relation to symptomatic and preclinical AD (Rijal Upadhaya et al., 2014). Thus, distinct biochemical stages of disease progression might have an influence on the clinical and pathological phenotype of AD patients, as well. To investigate a potential relationship of the structural differences in the SAD cohort with biochemical aspects, such as the Aβ load or the Aβ42/40 ratio, a correlation analysis with the LCO data was performed. No correlation between the LCO ratio and the Aβ load or Aβ42/40 ratio was detected. Risk factors like the age or ApoE genotype are thought to account for part of the phenotypic heterogeneity in SAD patients (Lahiri et al., 2004). Thus, we also investigated a correlation between the age of the patients as well as the ApoE genotype and the LCO data, but found no significant correlations. Finally, a potential degradation effect caused by a prolonged PMI, which might influence the structural properties of the tissue, was assessed, but no correlation between our structural data and the PMI was detected. Conclusively, the spectral results suggest conformational differences for Aβ pathology between FAD and SAD cases and remarkably also between distinct SAD patients. However, in order to confirm a strain-like paradigm for the human plaque pathology further experiments are needed. Such experiments should include the transmission of the aggregates to a susceptible host system, where it is anticipated that the different conformations are preserved if the strain principle applies for the investigated deposits (Aguzzi et al., 2007, Collinge and Clarke, 2007). The spectral data of the SAD cohort did not correlate with biochemical characteristics or established risk factors in our study, although a potential correlation cannot be excluded for a larger or differential cohort of AD patients. Nevertheless, these results suggest that the plaque conformation stays largely unaffected by general factors addressing the whole body or system suggesting that the initial seed formation or direct interactions of other cells on the plaque might predominantly influence the final plaque arrangement.

A sensible future step would be to correlate these conformational differences to the clinical phenotype in the AD patients. So far, the existence of significant

correlations between variations in structural features and variations in amyloid diseases has not been shown in humans (Tycko, 2015). However, such correlations could have diverse implications, as any correlations between Aβ fibril structures and the clinical progression in AD would favor the idea that amyloid fibrils have clinically relevant neurotoxic effects (Chetelat et al., 2012). Other studies however showed that some humans with substantial Aβ deposition in the brain do not show any clinical signs of AD (Gu et al., 2015) and that the amyloid load per se cannot predict the cognitive status in AD patients (Giannakopoulos et al., 2003). On the background that distinct predominant Aβ fibril structures can develop in different AD patients (Lu et al., 2013), these variations raise the important question of whether this polymorphism correlates with and even causes differences in neuronal toxicities, binding stoichiometry of imaging agents, and AD symptoms. In consequence, the amyloid diversity may potentially explain part of the discrepancy seen before.

We approached the question whether conformational differences can be detected among AD patients with novel, conformation-sensitive LCO dyes. LCOs are nowadays established as a valuable tool to detect and distinguish between amyloid lesions in mouse models of β-amyloidosis and on human post-mortem tissue (Aslund et al., 2009b, Klingstedt et al., 2011, Wegenast-Braun et al., 2012, Klingstedt et al., 2013, Shirani et al., 2015). In this thesis they were shown for the first time to successfully distinguish between Aβ conformers in a larger cohort of human AD brain sections. It is our aspiration that this work will pave the way towards the development of novel structure-specific imaging and treatment compounds for amyloid diseases, an especially important goal in light of potential correlations between amyloid structure and clinical phenotype. Only recently, pentameric LCOs have been introduced as successful anti-prion compounds in tg mice (Herrmann et al., 2015). In AD patients, Aβ-binding compounds like PIB are used routinely for PET in research and clinical practice (Klunk et al., 2004, Fleisher et al., 2011). The molecular-level binding sites for these compounds are currently under investigation (Fosso et al., 2016, LeVine and Walker, 2016) and differences in ligand binding, that are known for PIB in human AD (Rosen et al., 2010), may

also relate to structural amyloid variations and support the need for novel agents that selectively bind distinct amyloid structures. A specific goal should be to develop compounds that direct the aggregation process away from certain structures and towards others. Assuming, that certain structures lead more aggressively to the neurodegeneration in AD patients, the clearance of those conformers could be used to prevent or limit the disease process in those patients (Tycko, 2015).

In conclusion, a better understanding of the structural diversity of Aβ aggregates could provide important clues to the pathogenesis of AD and thereby also suggest new therapeutic approaches to the disease. The conformation-sensitive LCO tools open up a new way of investigating features of the disease that couldn't be assessed via classical methods so far, which might ultimately be used to discern benign from toxic aggregates. Once this technology is established it could be intended for imaging, diagnosis or even treatment of many neurodegenerative diseases.

References

Aguzzi A, Heikenwalder M, Polymenidou M (2007) Insights into prion strains and neurotoxicity. Nat Rev Mol Cell Biol 8:552-561.

Alzheimer A (1907) Über eine eigenartige Erkrankung der Hirnrinde. Allgemeine Zeitschrift für Psychatrie 64:146-148.

Alzheimer A (1911) Über eigenartige Krankheitsfälle des späteren Alters. Zeitschrift für die gesamte Neurologie und Psychiatrie 4:356-385.

Alzheimer's-Association (2015) 2015 Alzheimer's disease facts and figures. Alzheimer's & Dementia 11:332-384.

Aslund A, Herland A, Hammarstrom P, Nilsson KP, Jonsson BH, Inganas O, Konradsson P (2007) Studies of luminescent conjugated polythiophene derivatives: enhanced spectral discrimination of protein conformational states. Bioconjugate chemistry 18:1860-1868.

Aslund A, Nilsson KP, Konradsson P (2009a) Fluorescent oligo and poly-thiophenes and their utilization for recording biological events of diverse origin-when organic chemistry meets biology. J Chem Biol 2:161-175.

Aslund A, Sigurdson CJ, Klingstedt T, Grathwohl S, Bolmont T, Dickstein DL, Glimsdal E, Prokop S, Lindgren M, Konradsson P, Holtzman DM, Hof PR, Heppner FL, Gandy S, Jucker M, Aguzzi A, Hammarstrom P, Nilsson KP (2009b) Novel pentameric thiophene derivatives for in vitro and in vivo optical imaging of a plethora of protein aggregates in cerebral amyloidoses. ACS chemical biology 4:673-684.

Astbury WT, Dickinson S, Bailey K (1935) The X-ray interpretation of denaturation and the structure of the seed globulins. The Biochemical journal 29:2351-2360.

Bauer HH, Aebi U, Häner M, Hermann R, Müller M, Arvinte T, Merkle HP (1995) Architecture and Polymorphism of Fibrillar Supramolecular Assemblies Produced by in Vitro Aggregation of Human Calcitonin. Journal of structural biology 115:1-15.

Bennhold H (1922) Eine spezifische Amyloidfärbung mit Kongorot. Münch Med Wochenschr 69:1537-1538.

Bessen RA, Marsh RF (1994) Distinct PrP properties suggest the molecular basis of strain variation in transmissible mink encephalopathy. Journal of virology 68:7859-7868.

Braak H, Braak E (1991) Neuropathological stageing of Alzheimer-related changes. Acta neuropathologica 82:239-259.

Branden C, Tooze J (1999) Introduction to protein structure. Book Garaland Publishing 2nd edition.

Brown P, Gibbs CJ, Jr., Gajdusek DC, Cathala F, LaBauge R (1986) Transmission of Creutzfeldt-Jakob disease from formalin-fixed, paraffin-embedded human brain tissue. The New England journal of medicine 315:1614-1615.

Calhoun ME, Burgermeister P, Phinney AL, Stalder M, Tolnay M, Wiederhold KH, Abramowski D, Sturchler-Pierrat C, Sommer B, Staufenbiel M, Jucker M (1999) Neuronal overexpression of mutant amyloid precursor protein results in prominent deposition of cerebrovascular amyloid. Proc Natl Acad Sci U S A 96:14088-14093.

Calhoun ME, Wiederhold KH, Abramowski D, Phinney AL, Probst A, Sturchler-Pierrat C, Staufenbiel M, Sommer B, Jucker M (1998) Neuron loss in APP transgenic mice. Nature 395:755-756.

Chetelat G, Villemagne VL, Villain N, Jones G, Ellis KA, Ames D, Martins RN, Masters CL, Rowe CC (2012) Accelerated cortical atrophy in cognitively normal elderly with high beta-amyloid deposition. Neurology 78:477-484.

Chiti F, Dobson CM (2006) Protein misfolding, functional amyloid, and human disease. Annual review of biochemistry 75:333-366.

Chow VW, Mattson MP, Wong PC, Gleichmann M (2010) An overview of APP processing enzymes and products. Neuromolecular medicine 12:1-12.

Clavaguera F, Akatsu H, Fraser G, Crowther RA, Frank S, Hench J, Probst A, Winkler DT, Reichwald J, Staufenbiel M, Ghetti B, Goedert M, Tolnay M (2013) Brain homogenates from human tauopathies induce tau inclusions in mouse brain. Proceedings of the National Academy of Sciences of the United States of America 110:9535-9540.

Cohen AS, Calkins E (1959) Electron microscopic observations on a fibrous component in amyloid of diverse origins. Nature 183:1202-1203.

Cohen FE, Prusiner SB (1998) Pathologic conformations of prion proteins. Annual review of biochemistry 67:793-819.

Cohen M, Appleby B, Safar JG (2016) Distinct prion-like strains of amyloid beta implicated in phenotypic diversity of Alzheimer's disease. Prion 10:9-17.

Cohen ML, Kim C, Haldiman T, ElHag M, Mehndiratta P, Pichet T, Lissemore F, Shea M, Cohen Y, Chen W, Blevins J, Appleby BS, Surewicz K, Surewicz WK, Sajatovic M, Tatsuoka C, Zhang S, Mayo P, Butkiewicz M, Haines JL, Lerner AJ, Safar JG (2015) Rapidly progressive Alzheimer's disease features distinct structures of amyloid-beta. Brain : a journal of neurology 138:1009-1022.

Collinge J, Clarke AR (2007) A general model of prion strains and their pathogenicity. Science 318:930-936.

Corder EH, Saunders AM, Strittmatter WJ, Schmechel DE, Gaskell PC, Small GW, Roses AD, Haines JL, Pericak-Vance MA (1993) Gene dose of apolipoprotein E type 4 allele and the risk of Alzheimer's disease in late onset families. Science 261:921-923.

De Kimpe L, Scheper W (2010) From alpha to omega with Abeta: targeting the multiple molecular appearances of the pathogenic peptide in Alzheimer's disease. Current medicinal chemistry 17:198-212.

De Strooper B (2007) Loss-of-function presenilin mutations in Alzheimer disease. Talking Point on the role of presenilin mutations in Alzheimer disease. EMBO Rep 8:141-146.

DeArmond SJ, Prusiner SB (1995) Etiology and pathogenesis of prion diseases. Am J Pathol 146:785-811.

Delrue I, Verzele D, Madder A, Nauwynck HJ (2012) Inactivated virus vaccines from chemistry to prophylaxis: merits, risks and challenges. Expert Review of Vaccines 11:695-719.

Di Fede G, Giaccone G, Tagliavini F (2013) Hereditary and sporadic beta-amyloidoses. Frontiers in bioscience (Landmark edition) 18:1202-1226.

Eanes ED, Glenner GG (1968) X-ray diffraction studies on amyloid filaments. The journal of histochemistry and cytochemistry : official journal of the Histochemistry Society 16:673-677.

Eckman CB, Mehta ND, Crook R, Perez-tur J, Prihar G, Pfeiffer E, Graff-Radford N, Hinder P, Yager D, Zenk B, Refolo LM, Prada CM, Younkin SG, Hutton M, Hardy J (1997) A new pathogenic mutation in the APP gene (I716V) increases the relative proportion of A beta 42(43). Human molecular genetics 6:2087-2089.

Edbauer D, Winkler E, Regula JT, Pesold B, Steiner H, Haass C (2003) Reconstitution of gamma-secretase activity. Nature cell biology 5:486-488.

Eisele YS, Bolmont T, Heikenwalder M, Langer F, Jacobson LH, Yan ZX, Roth K, Aguzzi A, Staufenbiel M, Walker LC, Jucker M (2009) Induction of cerebral beta-amyloidosis: intracerebral versus systemic Abeta inoculation. Proceedings of the National Academy of Sciences of the United States of America 106:12926-12931.

Eisele YS, Fritschi SK, Hamaguchi T, Obermuller U, Fuger P, Skodras A, Schafer C, Odenthal J, Heikenwalder M, Staufenbiel M, Jucker M (2014) Multiple factors contribute to the peripheral induction of cerebral beta-amyloidosis. The Journal of neuroscience : the official journal of the Society for Neuroscience 34:10264-10273.

Eisele YS, Obermuller U, Heilbronner G, Baumann F, Kaeser SA, Wolburg H, Walker LC, Staufenbiel M, Heikenwalder M, Jucker M (2010) Peripherally applied Abeta-containing inoculates induce cerebral beta-amyloidosis. Science 330:980-982.

Eisenberg D, Jucker M (2012) The amyloid state of proteins in human diseases. Cell 148:1188-1203.

Esch FS, Keim PS, Beattie EC, Blacher RW, Culwell AR, Oltersdorf T, McClure D, Ward PJ (1990) Cleavage of amyloid beta peptide during constitutive processing of its precursor. Science 248:1122-1124.

Estrada LD, Soto C (2007) Disrupting beta-amyloid aggregation for Alzheimer disease treatment. Current topics in medicinal chemistry 7:115-126.

Finckh U, Muller-Thomsen T, Mann U, Eggers C, Marksteiner J, Meins W, Binetti G, Alberici A, Hock C, Nitsch RM, Gal A (2000) High prevalence of pathogenic mutations in patients with early-onset dementia detected by sequence analyses of four different genes. American journal of human genetics 66:110-117.

Fleisher AS, Chen K, Liu X, Roontiva A, Thiyyagura P, Ayutyanont N, Joshi AD, Clark CM, Mintun MA, Pontecorvo MJ, Doraiswamy PM, Johnson KA, Skovronsky DM, Reiman EM (2011) Using positron emission tomography and florbetapir F18 to image cortical amyloid in patients with mild cognitive impairment or dementia due to Alzheimer disease. Archives of neurology 68:1404-1411.

Forman MS, Trojanowski JQ, Lee VM (2004) Neurodegenerative diseases: a decade of discoveries paves the way for therapeutic breakthroughs. Nat Med 10:1055-1063.

Fosso MY, McCarty K, Head E, Garneau-Tsodikova S, LeVine H, 3rd (2016) Differential Effects of Structural Modifications on the Competition of Chalcones for the PIB Amyloid Imaging Ligand-Binding Site in Alzheimer's Disease Brain and Synthetic Abeta Fibrils. ACS chemical neuroscience 7:171-176.

Fox CH, Johnson FB, Whiting J, Roller PP (1985) Formaldehyde fixation. The journal of histochemistry and cytochemistry : official journal of the Histochemistry Society 33:845-853.

Fritschi SK, Cintron A, Ye L, Mahler J, Buhler A, Baumann F, Neumann M, Nilsson KP, Hammarstrom P, Walker LC, Jucker M (2014) Abeta seeds resist inactivation by formaldehyde. Acta neuropathologica 128:477-484.

Frost B, Diamond MI (2010) Prion-like mechanisms in neurodegenerative diseases. Nature reviews Neuroscience 11:155-159.

Fung J, Frost D, Chakrabartty A, McLaurin J (2004) Interaction of human and mouse Abeta peptides. J Neurochem 91:1398-1403.

Giannakopoulos P, Herrmann FR, Bussiere T, Bouras C, Kovari E, Perl DP, Morrison JH, Gold G, Hof PR (2003) Tangle and neuron numbers, but not amyloid load, predict cognitive status in Alzheimer's disease. Neurology 60:1495-1500.

Glenner GG, Wong CW (1984) Alzheimer's disease: initial report of the purification and characterization of a novel cerebrovascular amyloid protein. Biochemical and biophysical research communications 120:885-890.

Goate A, Chartier-Harlin MC, Mullan M, Brown J, Crawford F, Fidani L, Giuffra L, Haynes A, Irving N, James L, et al. (1991) Segregation of a missense mutation in the amyloid precursor protein gene with familial Alzheimer's disease. Nature 349:704-706.

Goedert M, Clavaguera F, Tolnay M (2010) The propagation of prion-like protein inclusions in neurodegenerative diseases. Trends in neurosciences 33:317-325.

Goedert M, Spillantini MG (2006) A century of Alzheimer's disease. Science 314:777-781.

Goldgaber D, Lerman MI, McBride OW, Saffiotti U, Gajdusek DC (1987) Characterization and chromosomal localization of a cDNA encoding brain amyloid of Alzheimer's disease. Science 235:877-880.

Gu Y, Razlighi QR, Zahodne LB, Janicki SC, Ichise M, Manly JJ, Devanand DP, Brickman AM, Schupf N, Mayeux R, Stern Y (2015) Brain Amyloid Deposition and Longitudinal Cognitive Decline in Nondemented Older Subjects: Results from a Multi-Ethnic Population. PloS one 10:e0123743.

Guo JL, Covell DJ, Daniels JP, Iba M, Stieber A, Zhang B, Riddle DM, Kwong LK, Xu Y, Trojanowski JQ, Lee VM (2013) Distinct alpha-synuclein strains differentially promote tau inclusions in neurons. Cell 154:103-117.

Haass C, Kaether C, Thinakaran G, Sisodia S (2012) Trafficking and proteolytic processing of APP. Cold Spring Harbor perspectives in medicine 2:a006270.

Hardy J, Allsop D (1991) Amyloid deposition as the central event in the aetiology of Alzheimer's disease. Trends in pharmacological sciences 12:383-388.

Hardy J, Mullan M, Chartier-Harlin MC, Brown J, Goate A, al. e (1991) Molecular classification of Alzheimer's disease. The Lancet 337:1342-1343.

Hardy J, Selkoe DJ (2002) The amyloid hypothesis of Alzheimer's disease: progress and problems on the road to therapeutics. Science 297:353-356.

Hardy JA, Higgins GA (1992) Alzheimer's disease: the amyloid cascade hypothesis. Science 256:184-185.

Hefendehl JK, Wegenast-Braun BM, Liebig C, Eicke D, Milford D, Calhoun ME, Kohsaka S, Eichner M, Jucker M (2011) Long-term in vivo imaging of beta-amyloid plaque appearance and growth in a mouse model of cerebral beta-amyloidosis. The Journal of neuroscience : the official journal of the Society for Neuroscience 31:624-629.

Heilbronner G, Eisele YS, Langer F, Kaeser SA, Novotny R, Nagarathinam A, Aslund A, Hammarstrom P, Nilsson KP, Jucker M (2013) Seeded strain-like transmission of beta-amyloid morphotypes in APP transgenic mice. EMBO Rep 14:1017-1022.

Herrmann US, Schutz AK, Shirani H, Huang D, Saban D, Nuvolone M, Li B, Ballmer B, Aslund AK, Mason JJ, Rushing E, Budka H, Nystrom S, Hammarstrom P, Bockmann A, Caflisch A, Meier BH, Nilsson KP, Hornemann S, Aguzzi A (2015) Structure-based drug design identifies polythiophenes as antiprion compounds. Science translational medicine 7:299ra123.

Ho HA, Boissinot M, Bergeron MG, Corbeil G, Dore K, Boudreau D, Leclerc M (2002) Colorimetric and fluorometric detection of nucleic acids using cationic polythiophene derivatives. Angewandte Chemie 41:1548-1551.

Holtzman DM, Herz J, Bu G (2012) Apolipoprotein E and apolipoprotein E receptors: normal biology and roles in Alzheimer disease. Cold Spring Harbor perspectives in medicine 2:a006312.

Howie AJ (2015) "Green (or apple-green) birefringence" of Congo red-stained amyloid. Amyloid : the international journal of experimental and clinical investigation : the official journal of the International Society of Amyloidosis 22:205-206.

Howie AJ, Brewer DB, Howell D, Jones AP (2008) Physical basis of colors seen in Congo red-stained amyloid in polarized light. Laboratory investigation; a journal of technical methods and pathology 88:232-242.

Jankowsky JL, Younkin LH, Gonzales V, Fadale DJ, Slunt HH, Lester HA, Younkin SG, Borchelt DR (2007) Rodent A beta modulates the solubility and distribution of amyloid deposits in transgenic mice. J Biol Chem 282:22707-22720.

Janocko NJ, Brodersen KA, Soto-Ortolaza AI, Ross OA, Liesinger AM, Duara R, Graff-Radford NR, Dickson DW, Murray ME (2012) Neuropathologically defined subtypes of Alzheimer's disease differ significantly from neurofibrillary tangle-predominant dementia. Acta neuropathologica 124:681-692.

Jarrett JT, Berger EP, Lansbury PT, Jr. (1993) The carboxy terminus of the beta amyloid protein is critical for the seeding of amyloid formation: implications for the pathogenesis of Alzheimer's disease. Biochemistry 32:4693-4697.

Jarrett JT, Lansbury PT, Jr. (1993) Seeding "one-dimensional crystallization" of amyloid: a pathogenic mechanism in Alzheimer's disease and scrapie? Cell 73:1055-1058.

Jimenez JL, Guijarro JI, Orlova E, Zurdo J, Dobson CM, Sunde M, Saibil HR (1999) Cryo-electron microscopy structure of an SH3 amyloid fibril and model of the molecular packing. The EMBO journal 18:815-821.

Jucker M (2010) The benefits and limitations of animal models for translational research in neurodegenerative diseases. Nat Med 16:1210-1214.

Jucker M, Walker LC (2013) Self-propagation of pathogenic protein aggregates in neurodegenerative diseases. Nature 501:45-51.

Kang J, Lemaire HG, Unterbeck A, Salbaum JM, Masters CL, Grzeschik KH, Multhaup G, Beyreuther K, Muller-Hill B (1987) The precursor of Alzheimer's disease amyloid A4 protein resembles a cell-surface receptor. Nature 325:733-736.

Klingstedt T, Aslund A, Simon RA, Johansson LB, Mason JJ, Nystrom S, Hammarstrom P, Nilsson KP (2011) Synthesis of a library of oligothiophenes and their utilization as fluorescent ligands for spectral assignment of protein aggregates. Org Biomol Chem 9:8356-8370.

Klingstedt T, Blechschmidt C, Nogalska A, Prokop S, Haggqvist B, Danielsson O, Engel WK, Askanas V, Heppner FL, Nilsson KP (2013) Luminescent conjugated oligothiophenes for sensitive fluorescent assignment of protein inclusion bodies. Chembiochem : a European journal of chemical biology 14:607-616.

Klingstedt T, Nilsson KP (2012) Luminescent conjugated poly- and oligo-thiophenes: optical ligands for spectral assignment of a plethora of protein aggregates. Biochem Soc Trans 40:704-710.

Klunk WE, Bacskai BJ, Mathis CA, Kajdasz ST, McLellan ME, Frosch MP, Debnath ML, Holt DP, Wang Y, Hyman BT (2002) Imaging Abeta plaques in living transgenic mice with multiphoton microscopy and methoxy-X04, a systemically administered Congo red derivative. Journal of neuropathology and experimental neurology 61:797-805.

Klunk WE, Engler H, Nordberg A, Wang Y, Blomqvist G, Holt DP, Bergstrom M, Savitcheva I, Huang GF, Estrada S, Ausen B, Debnath ML, Barletta J, Price JC, Sandell J, Lopresti BJ, Wall A, Koivisto P, Antoni G, Mathis CA, Langstrom B (2004) Imaging brain amyloid in Alzheimer's disease with Pittsburgh Compound-B. Annals of neurology 55:306-319.

Klunk WE, Lopresti BJ, Ikonomovic MD, Lefterov IM, Koldamova RP, Abrahamson EE, Debnath ML, Holt DP, Huang G-f, Shao L, DeKosky ST, Price JC, Mathis CA (2005) Binding of the Positron Emission Tomography Tracer Pittsburgh Compound-B Reflects the Amount of Amyloid-β in Alzheimer's Disease Brain But Not in Transgenic Mouse Brain. The Journal of Neuroscience 25:10598-10606.

Kosik KS, Joachim CL, Selkoe DJ (1986) Microtubule-associated protein tau (tau) is a major antigenic component of paired helical filaments in Alzheimer disease. Proceedings of the National Academy of Sciences of the United States of America 83:4044-4048.

Kraepelin E (1910) Ein Lehrbuch für Studierende und Ärzte. Psychiatrie II 8.

Kuo Y-M, Kokjohn TA, Beach TG, Sue LI, Brune D, Lopez JC, Kalback WM, Abramowski D, Sturchler-Pierrat C, Staufenbiel M, Roher AE (2001) Comparative Analysis of Amyloid-β Chemical Structure and Amyloid Plaque Morphology of Transgenic Mouse and Alzheimer's Disease Brains. Journal of Biological Chemistry 276:12991-12998.

Kyle RA (2001) Amyloidosis: a convoluted story. British journal of haematology 114:529-538.

Lahiri DK, Sambamurti K, Bennett DA (2004) Apolipoprotein gene and its interaction with the environmentally driven risk factors: molecular, genetic and epidemiological studies of Alzheimer's disease. Neurobiol Aging 25:651-660.

Langer F, Eisele YS, Fritschi SK, Staufenbiel M, Walker LC, Jucker M (2011) Soluble Abeta seeds are potent inducers of cerebral beta-amyloid deposition. The Journal of neuroscience : the official journal of the Society for Neuroscience 31:14488-14495.

Larner AJ, Doran M (2006) Clinical phenotypic heterogeneity of Alzheimer's disease associated with mutations of the presenilin-1 gene. Journal of neurology 253:139-158.

Leclerc M (1999) Optical and electrochemical transducers based on functionalized conjugated polymers. Advanced Materials 11:1491-+.

Lee J, Culyba EK, Powers ET, Kelly JW (2011) Amyloid-beta forms fibrils by nucleated conformational conversion of oligomers. Nature chemical biology 7:602-609.

LeVine H, 3rd (1993) Thioflavine T interaction with synthetic Alzheimer's disease beta-amyloid peptides: detection of amyloid aggregation in solution. Protein science : a publication of the Protein Society 2:404-410.

Levine H, 3rd, Walker LC (2010) Molecular polymorphism of Abeta in Alzheimer's disease. Neurobiol Aging 31:542-548.

LeVine H, 3rd, Walker LC (2016) What amyloid ligands can tell us about molecular polymorphism and disease. Neurobiol Aging 42:205-212.

Levy-Lahad E, Wasco W, Poorkaj P, Romano DM, Oshima J, Pettingell WH, Yu CE, Jondro PD, Schmidt SD, Wang K, et al. (1995) Candidate gene for the chromosome 1 familial Alzheimer's disease locus. Science 269:973-977.

Lord A, Philipson O, Klingstedt T, Westermark G, Hammarström P, Nilsson KPR, Nilsson LNG (2011) Observations in APP Bitransgenic Mice Suggest that Diffuse and Compact Plaques Form via Independent Processes in Alzheimer's Disease. The American Journal of Pathology 178:2286-2298.

Lu JX, Qiang W, Yau WM, Schwieters CD, Meredith SC, Tycko R (2013) Molecular structure of beta-amyloid fibrils in Alzheimer's disease brain tissue. Cell 154:1257-1268.

Maarouf CL, Daugs ID, Spina S, Vidal R, Kokjohn TA, Patton RL, Kalback WM, Luehrs DC, Walker DG, Castano EM, Beach TG, Ghetti B, Roher AE (2008) Histopathological and molecular heterogeneity among individuals with dementia associated with Presenilin mutations. Molecular neurodegeneration 3:20.

Mahler J, Morales-Corraliza J, Stolz J, Skodras A, Radde R, Duma CC, Eisele YS, Mazzella MJ, Wong H, Klunk WE, Nilsson KP, Staufenbiel M, Mathews PM, Jucker M, Wegenast-Braun BM (2015) Endogenous murine Abeta increases amyloid deposition in APP23 but not in APPPS1 transgenic mice. Neurobiol Aging 36:2241-2247.

Manton KC, Gu XL, Ukraintseva SV (2005) Declining prevalence of dementia in the U.S. elderly population. Advances in gerontology = Uspekhi gerontologii / Rossiiskaia akademiia nauk, Gerontologicheskoe obshchestvo 16:30-37.

Masters CL, Simms G, Weinman NA, Multhaup G, McDonald BL, Beyreuther K (1985) Amyloid plaque core protein in Alzheimer disease and Down syndrome. Proceedings of the National Academy of Sciences of the United States of America 82:4245-4249.

Mattsson N, Schott JM, Hardy J, Turner MR, Zetterberg H (2016) Selective vulnerability in neurodegeneration: insights from clinical variants of Alzheimer's disease. Journal of neurology, neurosurgery, and psychiatry.

Mayeux R (2003) Epidemiology of neurodegeneration. Annual review of neuroscience 26:81-104.

Meyer-Luehmann M, Coomaraswamy J, Bolmont T, Kaeser S, Schaefer C, Kilger E, Neuenschwander A, Abramowski D, Frey P, Jaton AL, Vigouret JM, Paganetti P, Walsh DM, Mathews PM, Ghiso J, Staufenbiel M, Walker LC, Jucker M (2006) Exogenous induction of cerebral beta-amyloidogenesis is governed by agent and host. Science 313:1781-1784.

Morales-Corraliza J, Mazzella MJ, Berger JD, Diaz NS, Choi JHK, Levy E, Matsuoka Y, Planel E, Mathews PM (2009) *In Vivo* Turnover of Tau and APP Metabolites in the Brains of Wild-Type and Tg2576 Mice: Greater Stability of sAPP in the ?-Amyloid Depositing Mice. PloS one 4:e7134.

Morales-Corraliza J, Schmidt SD, Mazzella MJ, Berger JD, Wilson DA, Wesson DW, Jucker M, Levy E, Nixon RA, Mathews PM (2013) Immunization targeting a minor plaque constituent clears beta-amyloid and rescues behavioral deficits in an Alzheimer's disease mouse model. Neurobiology of aging 34:137-145.

Morgan C, Colombres M, Nunez MT, Inestrosa NC (2004) Structure and function of amyloid in Alzheimer's disease. Progress in neurobiology 74:323-349.

Morris GP, Clark IA, Vissel B (2014) Inconsistencies and controversies surrounding the amyloid hypothesis of Alzheimer's disease. Acta neuropathologica communications 2:135.

Mulder GJ (1839) Über die Zusammensetzung einiger thierischer Substanzen. Journal für praktische Chemie 16:129-152.

Mullan M, Crawford F, Axelman K, Houlden H, Lilius L, Winblad B, Lannfelt L (1992) A pathogenic mutation for probable Alzheimer's disease in the APP gene at the N-terminus of beta-amyloid. Nature genetics 1:345-347.

Murrell J, Ghetti B, Cochran E, Macias-Islas MA, Medina L, Varpetian A, Cummings JL, Mendez MF, Kawas C, Chui H, Ringman JM (2006) The A431E mutation in PSEN1 causing familial Alzheimer's disease originating in Jalisco State, Mexico: an additional fifteen families. Neurogenetics 7:277-279.

Nilsson KP, Aslund A, Berg I, Nystrom S, Konradsson P, Herland A, Inganas O, Stabo-Eeg F, Lindgren M, Westermark GT, Lannfelt L, Nilsson LN, Hammarstrom P (2007) Imaging distinct conformational states of amyloid-beta fibrils in Alzheimer's disease using novel luminescent probes. ACS chemical biology 2:553-560.

Nilsson KP, Hammarstrom P, Ahlgren F, Herland A, Schnell EA, Lindgren M, Westermark GT, Inganas O (2006) Conjugated polyelectrolytes--conformation-sensitive optical probes for staining and characterization of amyloid deposits. Chembiochem : a European journal of chemical biology 7:1096-1104.

Nilsson KP, Rydberg J, Baltzer L, Inganas O (2003) Self-assembly of synthetic peptides control conformation and optical properties of a zwitterionic polythiophene derivative. Proceedings of the National Academy of Sciences of the United States of America 100:10170-10174.

Nilsson KPR, Hammarstrom P (2008) Luminescent conjugated polymers: Illuminating the dark matters of biology and pathology. Advanced Materials 20:2639-2645.

Nilsson KPR, Herland A, Hammarström P, Inganäs O (2005) Conjugated Polyelectrolytes: Conformation-Sensitive Optical Probes for Detection of Amyloid Fibril Formation. Biochemistry 44:3718-3724.

Novotny R, Langer F, Mahler J, Skodras A, Vlachos A, Wegenast-Braun BM, Kaeser SA, Neher JJ, Eisele YS, Pietrowski MJ, Nilsson KP, Deller T, Staufenbiel M, Heimrich B, Jucker M (2016) Conversion of Synthetic Abeta to In Vivo Active Seeds and Amyloid Plaque Formation in a Hippocampal Slice Culture Model. The Journal of neuroscience : the official journal of the Society for Neuroscience 36:5084-5093.

Nystrom S, Psonka-Antonczyk KM, Ellingsen PG, Johansson LB, Reitan N, Handrick S, Prokop S, Heppner FL, Wegenast-Braun BM, Jucker M, Lindgren M, Stokke BT, Hammarstrom P, Nilsson KP (2013) Evidence for age-dependent in vivo conformational rearrangement within Abeta amyloid deposits. ACS chemical biology 8:1128-1133.

O'Brien RJ, Wong PC (2011) Amyloid precursor protein processing and Alzheimer's disease. Annual review of neuroscience 34:185-204.

Pallares I, Ventura S (2016) Understanding and predicting protein misfolding and aggregation: Insights from proteomics. Proteomics.

Pan KM, Baldwin M, Nguyen J, Gasset M, Serban A, Groth D, Mehlhorn I, Huang Z, Fletterick RJ, Cohen FE, et al. (1993) Conversion of alpha-helices into beta-sheets features in the formation of the scrapie prion proteins. Proceedings of the National Academy of Sciences of the United States of America 90:10962-10966.

Pattison IH (1965) RESISTANCE OF THE SCRAPIE AGENT TO FORMALIN. Journal of comparative pathology 75:159-164.

Pattison IH (1972) Scrapie--a personal view. Journal of clinical pathology Supplement (Royal College of Pathologists) 6:110-114.

Pauling L, Corey RB (1951) Configuration of polypeptide chains. Nature 168:550-551.

Peelaerts W, Bousset L, Van der Perren A, Moskalyuk A, Pulizzi R, Giugliano M, Van den Haute C, Melki R, Baekelandt V (2015) alpha-Synuclein strains cause distinct synucleinopathies after local and systemic administration. Nature 522:340-344.

Petkova AT, Leapman RD, Guo Z, Yau WM, Mattson MP, Tycko R (2005) Self-propagating, molecular-level polymorphism in Alzheimer's beta-amyloid fibrils. Science 307:262-265.

Portelius E, Andreasson U, Ringman JM, Buerger K, Daborg J, Buchhave P, Hansson O, Harmsen A, Gustavsson MK, Hanse E, Galasko D, Hampel H, Blennow K, Zetterberg H (2010a) Distinct cerebrospinal fluid amyloid beta peptide signatures in sporadic and PSEN1 A431E-associated familial Alzheimer's disease. Molecular neurodegeneration 5:2.

Portelius E, Bogdanovic N, Gustavsson MK, Volkmann I, Brinkmalm G, Zetterberg H, Winblad B, Blennow K (2010b) Mass spectrometric characterization of brain amyloid beta isoform signatures in familial and sporadic Alzheimer's disease. Acta neuropathologica 120:185-193.

Portelius E, Zetterberg H, Gobom J, Andreasson U, Blennow K (2008) Targeted proteomics in Alzheimer's disease: focus on amyloid-beta. Expert review of proteomics 5:225-237.

Powers ET, Morimoto RI, Dillin A, Kelly JW, Balch WE (2009) Biological and chemical approaches to diseases of proteostasis deficiency. Annual review of biochemistry 78:959-991.

Prince M, Wimo A, Guerchet M, Ali G, Wu Y, Prina M (2015) World Alzheimer Report 2015. The global impact of dementia. An analysis of prevalence, incidence, cost and trends. Alzheimer's Disease International, London.

Prusiner SB (1982) Novel proteinaceous infectious particles cause scrapie. Science 216:136-144.

Prusiner SB (1998) Prions. Proceedings of the National Academy of Sciences 95:13363-13383.

Prusiner SB (2013) Biology and genetics of prions causing neurodegeneration. Annual review of genetics 47:601-623.

Puchtler (1962) On the binding of Congo Red by amyloid.

Pype S, Moechars D, Dillen L, Mercken M (2003) Characterization of amyloid beta peptides from brain extracts of transgenic mice overexpressing the London mutant of human amyloid precursor protein. J Neurochem 84:602-609.

Radde R, Bolmont T, Kaeser SA, Coomaraswamy J, Lindau D, Stoltze L, Calhoun ME, Jaggi F, Wolburg H, Gengler S, Haass C, Ghetti B, Czech C, Holscher C, Mathews PM, Jucker M (2006) Abeta42-driven cerebral amyloidosis in transgenic mice reveals early and robust pathology. EMBO Rep 7:940-946.

Rijal Upadhaya A, Kosterin I, Kumar S, von Arnim CA, Yamaguchi H, Fandrich M, Walter J, Thal DR (2014) Biochemical stages of amyloid-beta peptide aggregation and accumulation in the human brain and their association with symptomatic and pathologically preclinical Alzheimer's disease. Brain : a journal of neurology 137:887-903.

Ringman JM, Goate A, Masters CL, Cairns NJ, Danek A, Graff-Radford N, Ghetti B, Morris JC, Dominantly Inherited Alzheimer N (2014) Genetic heterogeneity in Alzheimer disease and implications for treatment strategies. Current neurology and neuroscience reports 14:499.

Robakis NK, Ramakrishna N, Wolfe G, Wisniewski HM (1987) Molecular cloning and characterization of a cDNA encoding the cerebrovascular and the neuritic plaque amyloid peptides. Proceedings of the National Academy of Sciences of the United States of America 84:4190-4194.

Roeber S, Muller-Sarnowski F, Kress J, Edbauer D, Kuhlmann T, Tuttelmann F, Schindler C, Winter P, Arzberger T, Muller U, Danek A, Kretzschmar HA (2015) Three novel presenilin 1 mutations marking the wide spectrum of age at onset and clinical patterns in familial Alzheimer's disease. Journal of neural transmission (Vienna, Austria : 1996) 122:1715-1719.

Rogaeva EA, Fafel KC, Song YQ, Medeiros H, Sato C, Liang Y, Richard E, Rogaev EI, Frommelt P, Sadovnick AD, Meschino W, Rockwood K, Boss MA, Mayeux R, St George-Hyslop P (2001) Screening for PS1 mutations in a referral-based series of AD cases: 21 novel mutations. Neurology 57:621-625.

Rosen RF, Ciliax BJ, Wingo TS, Gearing M, Dooyema J, Lah JJ, Ghiso JA, LeVine H, 3rd, Walker LC (2010) Deficient high-affinity binding of Pittsburgh compound B in a case of Alzheimer's disease. Acta neuropathologica 119:221-233.

Ross CA, Poirier MA (2004) Protein aggregation and neurodegenerative disease. Nat Med 10 Suppl:S10-17.

Safar J, Wille H, Itri V, Groth D, Serban H, Torchia M, Cohen FE, Prusiner SB (1998) Eight prion strains have PrP(Sc) molecules with different conformations. Nat Med 4:1157-1165.

Sanders DW, Kaufman SK, DeVos SL, Sharma AM, Mirbaha H, Li A, Barker SJ, Foley AC, Thorpe JR, Serpell LC, Miller TM, Grinberg LT, Seeley WW, Diamond MI (2014) Distinct tau prion strains propagate in cells and mice and define different tauopathies. Neuron 82:1271-1288.

Schrijvers EM, Verhaaren BF, Koudstaal PJ, Hofman A, Ikram MA, Breteler MM (2012) Is dementia incidence declining?: Trends in dementia incidence since 1990 in the Rotterdam Study. Neurology 78:1456-1463.

Selkoe DJ (2011) Alzheimer's disease. Cold Spring Harbor perspectives in biology 3.

Serpell LC, Sunde M, Benson MD, Tennent GA, Pepys MB, Fraser PE (2000) The protofilament substructure of amyloid fibrils. Journal of molecular biology 300:1033-1039.

Sherrington R, Rogaev EI, Liang Y, Rogaeva EA, Levesque G, Ikeda M, Chi H, Lin C, Li G, Holman K, Tsuda T, Mar L, Foncin JF, Bruni AC, Montesi MP, Sorbi S, Rainero I, Pinessi L, Nee L, Chumakov I, Pollen D, Brookes A, Sanseau P, Polinsky RJ, Wasco W, Da Silva HA, Haines JL, Perkicak-Vance MA, Tanzi RE, Roses AD, Fraser PE, Rommens JM, St George-Hyslop PH (1995) Cloning of a gene bearing missense mutations in early-onset familial Alzheimer's disease. Nature 375:754-760.

Shirahama T, Cohen AS (1967) High-resolution electron microscopic analysis of the amyloid fibril. The Journal of cell biology 33:679-708.

Shirani H, Linares M, Sigurdson CJ, Lindgren M, Norman P, Nilsson KP (2015) A Palette of Fluorescent Thiophene-Based Ligands for the Identification of Protein Aggregates. Chemistry 21:15133-15137.

Sigurdson CJ, Nilsson KP, Hornemann S, Manco G, Polymenidou M, Schwarz P, Leclerc M, Hammarstrom P, Wuthrich K, Aguzzi A (2007) Prion strain discrimination using luminescent conjugated polymers. Nature methods 4:1023-1030.

Simon RA, Shirani H, Aslund KO, Back M, Haroutunian V, Gandy S, Nilsson KP (2014) Pentameric thiophene-based ligands that spectrally discriminate amyloid-beta and tau aggregates display distinct solvatochromism and viscosity-induced spectral shifts. Chemistry 20:12537-12543.

Sipe JD, Benson MD, Buxbaum JN, Ikeda S, Merlini G, Saraiva MJ, Westermark P (2014) Nomenclature 2014: Amyloid fibril proteins and clinical classification of the amyloidosis. Amyloid : the international journal of experimental and clinical investigation : the official journal of the International Society of Amyloidosis 21:221-224.

Sipe JD, Cohen AS (2000) Review: history of the amyloid fibril. Journal of structural biology 130:88-98.

Sisodia SS (1992) Beta-amyloid precursor protein cleavage by a membrane-bound protease. Proceedings of the National Academy of Sciences of the United States of America 89:6075-6079.

Sisodia SS, Koo EH, Beyreuther K, Unterbeck A, Price DL (1990) Evidence that beta-amyloid protein in Alzheimer's disease is not derived by normal processing. Science 248:492-495.

Stefani M, Dobson CM (2003) Protein aggregation and aggregate toxicity: new insights into protein folding, misfolding diseases and biological evolution. Journal of molecular medicine 81:678-699.

Strittmatter WJ, Saunders AM, Schmechel D, Pericak-Vance M, Enghild J, Salvesen GS, Roses AD (1993) Apolipoprotein E: high-avidity binding to beta-amyloid and increased frequency of type 4 allele in late-onset familial Alzheimer disease. Proceedings of the National Academy of Sciences of the United States of America 90:1977-1981.

Sturchler-Pierrat C, Abramowski D, Duke M, Wiederhold K-H, Mistl C, Rothacher S, Ledermann B, Bürki K, Frey P, Paganetti PA, Waridel C, Calhoun ME, Jucker M, Probst A, Staufenbiel M, Sommer B (1997) Two amyloid precursor protein transgenic mouse models with Alzheimer disease-like pathology. Proceedings of the National Academy of Sciences of the United States of America 94:13287-13292.

Sunde M, Serpell LC, Bartlam M, Fraser PE, Pepys MB, Blake CC (1997) Common core structure of amyloid fibrils by synchrotron X-ray diffraction. Journal of molecular biology 273:729-739.

Tagliavini F, Giaccone G, Frangione B, Bugiani O (1988) Preamyloid deposits in the cerebral cortex of patients with Alzheimer's disease and nondemented individuals. Neuroscience letters 93:191-196.

Tanaka M, Collins SR, Toyama BH, Weissman JS (2006) The physical basis of how prion conformations determine strain phenotypes. Nature 442:585-589.

Tekirian TL, Saido TC, Markesbery WR, Russell MJ, Wekstein DR, Patel E, Geddes JW (1998) N-terminal heterogeneity of parenchymal and cerebrovascular Abeta deposits. Journal of neuropathology and experimental neurology 57:76-94.

Thal DR, Attems J, Ewers M (2014) Spreading of amyloid, tau, and microvascular pathology in Alzheimer's disease: findings from neuropathological and neuroimaging studies. Journal of Alzheimer's disease : JAD 42 Suppl 4:S421-429.

Thal DR, Rub U, Orantes M, Braak H (2002) Phases of A beta-deposition in the human brain and its relevance for the development of AD. Neurology 58:1791-1800.

Thinakaran G, Koo EH (2008) Amyloid precursor protein trafficking, processing, and function. The Journal of biological chemistry 283:29615-29619.

Tycko R (2011) Solid-state NMR studies of amyloid fibril structure. Annual review of physical chemistry 62:279-299.

Tycko R (2015) Amyloid polymorphism: structural basis and neurobiological relevance. Neuron 86:632-645.

Van Broeckhoven C, Haan J, Bakker E, Hardy JA, Van Hul W, Wehnert A, Vegter-Van der Vlis M, Roos RA (1990) Amyloid beta protein precursor gene and hereditary cerebral hemorrhage with amyloidosis (Dutch). Science 248:1120-1122.

van Groen T, Kiliaan AJ, Kadish I (2006a) Deposition of mouse amyloid beta in human APP/PS1 double and single AD model transgenic mice. Neurobiol Dis 23:653-662.

van Groen T, Kiliaan AJ, Kadish I (2006b) Deposition of mouse amyloid β in human APP/PS1 double and single AD model transgenic mice. Neurobiology of Disease 23:653-662.

Vassar PS, Culling CF (1959) Fluorescent stains, with special reference to amyloid and connective tissues. Archives of pathology 68:487-498.

Vigo-Pelfrey C, Lee D, Keim P, Lieberburg I, Schenk DB (1993) Characterization of beta-amyloid peptide from human cerebrospinal fluid. J Neurochem 61:1965-1968.

Virchow R (1854) Zur Cellulose-Frage. Virchows Arch Pathol Anat 6:416-426.

Walker LC, Callahan MJ, Bian F, Durham RA, Roher AE, Lipinski WJ (2002) Exogenous induction of cerebral beta-amyloidosis in betaAPP-transgenic mice. Peptides 23:1241-1247.

Walker LC, Jucker M (2015) Neurodegenerative diseases: expanding the prion concept. Annual review of neuroscience 38:87-103.

Warren JD, Fletcher PD, Golden HL (2012) The paradox of syndromic diversity in Alzheimer disease. Nature reviews Neurology 8:451-464.

Wegenast-Braun BM, Skodras A, Bayraktar G, Mahler J, Fritschi SK, Klingstedt T, Mason JJ, Hammarstrom P, Nilsson KP, Liebig C, Jucker M (2012) Spectral discrimination of cerebral amyloid lesions after peripheral application of luminescent conjugated oligothiophenes. Am J Pathol 181:1953-1960.

Yamada T, Sasaki H, Furuya H, Miyata T, Goto I, Sakaki Y (1987) Complementary DNA for the mouse homolog of the human amyloid beta protein precursor. Biochemical and biophysical research communications 149:665-671.

Yescas P, Huertas-Vazquez A, Villarreal-Molina MT, Rasmussen A, Tusie-Luna MT, Lopez M, Canizales-Quinteros S, Alonso ME (2006) Founder effect for the Ala431Glu mutation of the presenilin 1 gene causing early-onset Alzheimer's disease in Mexican families. Neurogenetics 7:195-200.

Yonetani M, Nonaka T, Masuda M, Inukai Y, Oikawa T, Hisanaga S, Hasegawa M (2009) Conversion of wild-type alpha-synuclein into mutant-type fibrils and its propagation in the presence of A30P mutant. The Journal of biological chemistry 284:7940-7950.

Yoshitake T, Kiyohara Y, Kato I, Ohmura T, Iwamoto H, Nakayama K, Ohmori S, Nomiyama K, Kawano H, Ueda K, et al. (1995) Incidence and risk factors of vascular dementia and Alzheimer's disease in a defined elderly Japanese population: the Hisayama Study. Neurology 45:1161-1168.

Common abbreviations

α-syn	α-synuclein
Aβ	amyloid beta
AD	Alzheimer's disease
AICD	APP intracellular domain
ANOVA	analysis of variance
APP	amyloid beta precursor protein
ApoE	apolipoprotein E
BBB	blood-brain barrier
BSE	Bovine spongiform encephalopathy
CAA	cerebral amyloid angiopathy
CJD	Creutzfeldt Jakob disease
CTF	C-terminal fragment
FAD	familial Alzheimer's disease
hFTAA	hepta-formyl thiophene acetic acid
ko	knock-out
LCO	luminescent conjugated oligothiophene
LCP	luminescent conjugated polythiophene
MFG	middle frontal gyrus
min	minutes
NMR	Nuclear magnetic resonance
OL	occipital lobe
PBS	Phosphate-buffered saline
PD	Parkinson's disease
PET	Positron emission tomography
pFTAA	penta-formyl thiophene acetic acid
PIB	Pittsburgh compound B
PSEN	presenilin
PrP	prion protein
qFTAA	quadro-formyl thiophene acetic acid
RT	Room temperature
SAD	sporadic Alzheimer's disease

SEM	standard error of the mean
SMTG	superior middle frontal gyrus
TBS	Tris-buffered saline
tg	transgenic
ThT	Thioflavin T
wt	wild-type

Curriculum Vitae and Bibliography

Name	Jasmin Mahler
Date of birth	24.07.1985
City of birth	Heidelberg, Germany
Citizenship	German

Education and Academic Degrees

09/2012 - present: Doctoral Thesis

PhD student in Neuroscience, Department of Cellular Neurology, Hertie Institute for Clinical Brain Research and Graduate Training Centre of Neuroscience, Tübingen. Advisor: Prof. Mathias Jucker. Titel: "Hidden variations of Alzheimer's pathology: Insight into the amyloid diversity using conformation-sensitive dyes".

07/2012 - 09/2012: Scientific assistance

Student assistant in the Department of Cellular Neurology, Hertie Institute for Clinical Brain Research, Tübingen. Advisor: Prof. Mathias Jucker.

09/2010 - 05/2012: Master in Neuroscience

Master course in Cellular and Molecular Neuroscience at the Graduate Training Centre, University of Tübingen. Advisor: Prof. Mathias Jucker. Master Thesis: "*Ex vivo* and *in vivo* analysis of protein aggregates in transgenic mouse models of cerebral amyloidosis using luminescent conjugated oligothiophenes".

10/2006 - 06/2009: Bachelor in Biology

Studies in Biology at the University of Erlangen-Nürnberg. Advisor: Prof. Wolfgang Kreis. Bachelor Thesis: "Ketosteroidisomerase in Digitalis lanata".

Publications

Hefendehl JK, LeDue J, Rhodes K, **Mahler J**, Murphy T, MacVicar B (2016). Mapping synaptic glutamate transporter dysfunction in vivo to regions surrounding Aβ plaques by iGluSnFR Two-Photon imaging. *Nature Communications*. *(accepted).*

Novotny R[*], Langer F[*], **Mahler J**, Skodras A, Vlachos A, Wegenast-Braun BM, Kaeser SA, Neher JJ, Eisele YS, Pietrowski MJ, Nilsson KP, Deller T, Staufenbiel M, Heimrich B, Jucker M (2016). Conversion of synthetic Aβ to *in vivo* active seeds and amyloid plaque formation in a hippocampal slice culture model. *Journal of Neuroscience*. *36(18), 5084-93.*

Klingstedt T, Shirani H, **Mahler J**, Wegenast-Braun BM , Nyström S, Goedert M, Jucker M, Nilsson KP (2015). Distinct Spacing Between Anionic Groups: An Essential Chemical Determinant for Achieving Thiophene-Based Ligands to Distinguish *β*-Amyloid or Tau Polymorphic Aggregates. *Chemistry – A European Journal*. *21(25), 9072-82.*

Mahler J, Morales-Corraliza J, Stolz J, Skodras A, Radde R, Duma CC, Eisele YS, Mazzella MJ, Wong H, Klunk WE, Nilsson KP, Staufenbiel M, Mathews PM, Jucker M, Wegenast-Braun BM (2015). Endogenous murine Aβ increases amyloid deposition in APP23 but not in APPPS1 transgenic mice. *Neurobiology of Aging*. *36(7), 2241-7.*

Fritschi SK*, Cintron A*, Ye L, **Mahler J**, Bühler A, Baumann F, Neumann M, Nilsson KP, Hammarström P, Walker LC, Jucker M (2014). Aβ seeds resist inactivation by formaldehyde. *Acta Neuropathologica*. *181(4), 477-84.*

Wegenast-Braun BM, Skodras A, Bayraktar G, **Mahler J**, Fritschi SK, Klingstedt T, Mason JJ, Hammarström P, Nilsson KP, Liebig C, Jucker M (2012). Spectral discrimination of cerebral amyloid lesions after peripheral application of luminescent conjugated oligothiophenes. *The American Journal of Pathology*. *181(6), 1953-60.*

Abstracts

Mahler J*, Rasmussen J*, Diamond MI, Nilsson KP, Walker LC, Oblak, AL, Ghetti B, Baumann F, Jucker M (2016). Conformationally distinct amyloid-β variants in human Alzheimer's disease brain. **Gordon Research Conference**, Girona, Spain. *(poster presentation).*

Mahler J*, Rasmussen J*, Diamond MI, Nilsson KP, Oblak, AL, Ghetti B, Walker LC, Baumann F, Jucker M (2015). Structurally distinct amyloid-β species among Alzheimer's disease patients – revisiting a Pittsburgh compound B-refractory case. **Society for Neuroscience Meeting**, Chicago, USA. *(poster presentation).*

Bacioglu M*, **Mahler J***, Schweighauser M*, Wegenast-Braun B, Nilsson KP, Schell H, Shimshek DR, Kahle PJ, Eisele YS, Jucker M (2015). Strain-like fingerprints of α-synuclein inclusions in transgenic mouse lines. **EMBO-EMBL Meeting: Mechanisms of Neurodegeneration**, Heidelberg, Germany. *(poster presentation).*

* contributed equally